



Validation of SCIAMACHY limb NO₂ profiles using solar occultation measurements

R. Bauer¹, A. Rozanov¹, C. A. McLinden², L. L. Gordley³, W. Lotz¹, J. M. Russell III⁴, K. A. Walker⁵, J. M. Zawodny⁶, A. Ladstätter-Weissenmayer¹, H. Bovensmann¹, and J. P. Burrows¹

¹Institute of Environmental Physics (IUP), University of Bremen, Bremen, Germany

²Air Quality Research Division, Environment Canada, Toronto, Ontario, Canada

³GATS, Inc., Newport News, Virginia, USA

⁴Department of Atmospheric and Planetary Sciences, Hampton University, Hampton, Virginia, USA

⁵Department of Physics, University of Toronto, Toronto, Ontario, Canada

⁶NASA Langley Research Center, Hampton, Virginia, USA

Correspondence to: R. Bauer (ralf.bauer@iup.physik.uni-bremen.de)

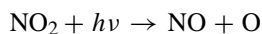
Received: 20 July 2011 – Published in Atmos. Meas. Tech. Discuss.: 28 July 2011

Revised: 19 April 2012 – Accepted: 24 April 2012 – Published: 14 May 2012

Abstract. The increasing amounts of reactive nitrogen in the stratosphere necessitate accurate global measurements of stratospheric nitrogen dioxide (NO₂). Over the past decade, the SCIAMACHY (SCanning Imaging Absorption spectroMeter for Atmospheric CHartography) instrument on ENVISAT (European Environmental Satellite) has been providing global coverage of stratospheric NO₂ every 6 days. In this study, the vertical distributions of NO₂ retrieved from SCIAMACHY limb measurements of the scattered solar light are validated by comparison with NO₂ products from three different satellite instruments (SAGE II, HALOE and ACE-FTS). The retrieval algorithm based on the information operator approach is discussed, and the sensitivity of the SCIAMACHY NO₂ limb retrievals is investigated. The photochemical corrections needed to make this validation feasible, and the chosen collocation criteria are described. For each instrument, a time period of two years is analyzed with several hundreds of collocation pairs for each year. As NO₂ is highly variable, the comparisons are performed for five latitudinal bins and four seasons. In the 20 to 40 km altitude range, mean relative differences between SCIAMACHY and other instruments are found to be typically within 20 to 30 %. The mean partial NO₂ columns in this altitude range agree typically within 15 % (both global monthly and zonal annual means). Larger differences are seen for SAGE II comparisons, which is consistent with the results presented by other authors. For SAGE II and ACE-FTS, the observed differences can be partially attributed to the diurnal effect error.

1 Introduction

As a minor constituent of the atmosphere, NO₂ is known for its influence on ozone concentrations. NO_x (the sum of NO and NO₂) is responsible for up to 70 % of the ozone loss in the stratosphere (see Crutzen, 1970; Portmann et al., 1999). The NO_x reactions dominate the catalytic ozone destruction between about 25 and 40 km:



While NO₂ participates in the destruction of ozone in the stratosphere, the same species leads to the formation of ozone in the troposphere, particularly during dense smog episodes. The major source for stratospheric NO₂ (hence, a cause of stratospheric ozone depletion) is nitrous oxide (N₂O) (see Montzka et al., 2011), an important greenhouse gas. It is also the most important ozone depleting substance not covered by the Montreal Protocol (Ravishankara et al., 2009). However, reduction of N₂O emission is a part of the Kyoto Protocol. In the troposphere, other sources of NO_x such as lightning events, fossil fuel combustion and biomass burning contribute to the NO₂ loading.

In this work, we investigate the performance of the SCIAMACHY NO₂ scientific retrieval processor (version 3.1) developed at the Institute of Environmental Physics, University of Bremen. Measurements from SCIAMACHY (SCanning

Imaging Absorption spectroMeter for Atmospheric CHar-tographY), a passive imaging spectrometer (Burrows et al., 1995; Bovensmann et al., 1999) on the European environmental satellite ENVISAT, are the basis for this investigation. The satellite instruments used for validation are the solar occultation instruments SAGE II (Stratospheric Aerosol Gas Experiment, Chu et al., 1989) on the Earth Radiation Budget Satellite (ERBS) of the NASA (National Aeronautics and Space Administration, USA), HALOE (Halogen Occultation Experiment, Russell III et al., 1993) on the US satellite UARS (Upper Atmosphere Research Satellite), and ACE-FTS (Atmospheric Chemistry Experiment-Fourier Transform Spectrometer, Walker et al., 2005; Bernath et al., 2005) on the Canadian satellite SCISAT-1. The SCIAMACHY results discussed here are retrieved from measurements of the scattered solar light in limb viewing geometry. While solar occultation instruments (including SCIAMACHY occultation mode) provide NO₂ distributions with a high accuracy, their spatial coverage is poor compared to that achieved in limb. Nevertheless, the solar occultation instruments still provide a significant number of retrieved NO₂ profiles, and a large number of comparisons have been performed. Due to the strong diurnal variation of NO₂, photochemical corrections need to be applied, as described in Sect. 2.3.

The first part of this work gives a description of the SCIAMACHY limb NO₂ retrieval, its sensitivity and error sources (including pointing, aerosols, clouds and diurnal effect error), and explains the photochemical model correction method used to match the measurements at different local times. The second part provides a short description of the occultation satellite instruments and the collocation criteria applied in this study, followed by a detailed discussion of the validation results.

2 SCIAMACHY limb observations

The SCIAMACHY instrument (Burrows et al., 1995; Bovensmann et al., 1999) on ENVISAT is a passive imaging spectrometer that comprises 8 spectral channels and covers a wide spectral range from 240 to 2400 nm. Each spectral channel is equipped with a grating spectrometer having a 1024 element diode array as a detector. For this study, only the measurements in spectral channel 3 ranging from 394 to 620 nm are used. This channel features a spectral resolution of 0.44 nm and a spectral sampling of 0.22 nm.

While SCIAMACHY measurements comprise three viewing modes, limb, nadir and occultation, only the limb geometry is discussed. In this study, SCIAMACHY observes in limb the atmosphere tangentially to the Earth's surface. The measurement begins at about 3 km below the horizon with the Earth still in the field of view, and continues vertically upwards to an altitude of about 100 km. At each tangent height, a horizontal scan of the duration of 1.5 s is performed followed by an elevation step of about 3.3 km with no

measurements, i.e. the vertical sampling is 3.3 km. The vertical instantaneous field of view of the SCIAMACHY instrument is about 2.5 km and the horizontal instantaneous field of view is 110 km at the tangent point. However, the horizontal resolution is mainly determined by the integration time during the horizontal scan resulting typically in a value of about 240 km.

In the 420 to 470 nm spectral range considered in this study, typical values of the signal to noise ratio for the spectra in limb measurements range from 3000 to 5000 at tangent heights between 20 and 30 km, decreasing to about 900 at 43 km. For more information about SCIAMACHY noise characteristics (see Noël et al., 1998).

Throughout this study, SCIAMACHY Level 1 data version 6.03 were used applying the calibration steps from 0 to 5, i.e. the wavelength calibration was performed and the corrections for memory effect, leakage current, pixel-to-pixel gain, etalon, and internal stray light were accounted for. The absolute radiometric calibration and polarization correction do not affect the retrieval results significantly because of the normalization by a limb measurement at an upper tangent height and a usage of the differential spectral structure, respectively. For this reason, these calibration steps were not applied.

2.1 SCIATRAN NO₂ limb retrieval

The SCIATRAN software package (Rozanov, 2012) is both a radiative transfer model and a retrieval algorithm that can be adjusted for a wide range of scientific tasks. It is used for NO₂ vertical profile retrieval from SCIAMACHY limb measurements as described below. In this study, version 3.1 of the NO₂ retrieval algorithm is used, which is based on SCIATRAN V2.2. Below, general retrieval settings for this version are described and the retrieval algorithm is presented. The SCIAMACHY NO₂ V3.1 data product includes also cloud masking flags from SCODA (SCIAMACHY cloud detection algorithm, Eichmann et al., 2009), see also von Savigny et al. (2005), which, however, have not been used in this study (see Sect. 2.4).

NO₂ retrieval as performed by version 3.1 of the retrieval processor works on the spectral range 420 to 470 nm and makes use of the differential absorption structure of NO₂. Also, O₃ is retrieved simultaneously, as it is the other important absorber in this spectral region, and O₄ is included in the forward model. The surface albedo is set to a constant value of 0.3. The selected tangent heights cover the range of about 10 to 40 km, while the reference tangent height, which is used to normalize the limb radiances, is about 43 km. The signal-to-noise ratio is estimated from the spectral residuals. Pressure and temperature information is taken from the ECMWF database and the NO₂ and O₃ cross sections from Bogumil et al. (1999) are used. A background aerosol scenario from LOWTRAN (Kneizys et al., 1988) is also included in the forward model. The forward model is initialized with a

climatological database (similar to Haley et al., 2004), which contains monthly averaged vertical profiles of O₃ and NO₂ on a 10°-latitude grid.

The general retrieval problem can be stated in this form:

$$\mathbf{y} = F(\mathbf{x}) + \varepsilon, \quad (1)$$

where F is the non-linear forward model operator, \mathbf{y} the data vector, \mathbf{x} the state vector and ε represents remaining errors. \mathbf{x} contains the atmospheric parameters to be retrieved, e.g. aerosol characteristics or molecular density profiles, like NO₂ vertical profiles. The data vector \mathbf{y} contains the information from all spectral points in the selected range for all used tangent heights. The reference tangent height is used as a background, i.e. the limb radiances are normalized with respect to the radiance at this tangent height. With this approach, the solar Fraunhofer structure is mostly eliminated as a problem, the instrument response function has much smaller influence, and no absolute calibration is needed. Furthermore, the effect of the instrument degradation over the years of operation in space upon the retrieval results is minimized.

The retrieval problem (Eq. 1) can be approximated as a linear model, as follows:

$$\mathbf{y} = \mathbf{y}_0 + \mathbf{K}_0(\mathbf{x} - \mathbf{x}_0) + \varepsilon. \quad (2)$$

Here, \mathbf{y}_0 is the measurement vector corresponding to the a priori profiles, \mathbf{x}_0 is the a priori state vector and \mathbf{K}_0 is a Jacobian matrix also referred to as the weighting function matrix. \mathbf{K}_0 is identified as

$$F(\mathbf{x}) \approx F(\mathbf{x}_0) + \left. \frac{\delta F}{\delta \mathbf{x}} \right|_{\mathbf{x}_0} (\mathbf{x} - \mathbf{x}_0) = F(\mathbf{x}_0) + \mathbf{K}_0(\mathbf{x} - \mathbf{x}_0). \quad (3)$$

The retrieval process is divided into two steps. The first is the pre-processing step, which is performed to eliminate most spectral features not associated with retrieval parameters. At this step, measurements at different tangent heights (with the exception of the reference tangent height) are processed independently. First, a third order polynomial is subtracted from the logarithms of the measurement spectra at each tangent height and the reference tangent height, and from the logarithms of the simulated spectra and from the weighting functions. This is done in order to minimize the influence of broadband instrument calibration errors and unknown scattering characteristics of the atmosphere. Then, a shift and squeeze correction and scaling factors for correction spectra (in this implementation: Ring spectra, undersampling and stray light correction) are obtained. Correction spectra are also called pseudoabsorbers. For more details see Sioris et al. (2003); Haley et al. (2004); Rozanov et al. (2005) and Rozanov et al. (2011). The measurement data are corrected using the results from the pre-processing step.

The aim of the second step in the retrieval process is to solve the full inverse problem. Computing the trace gas amounts from a set of measured spectra is far more difficult than generating spectra given a known set of trace gases and their absorption features. The radiative transfer equation describing the relation between radiance measured by the instrument and atmospheric parameter needs to be inverted.

To achieve this, the following quadratic form is minimized:

$$\left\| (\mathbf{y} - \mathbf{y}_0) - \mathbf{K}_0(\mathbf{x} - \mathbf{x}_0) \right\|_{\mathbf{S}_\varepsilon}^2 + \left\| (\mathbf{x} - \mathbf{x}_0) \right\|_{\mathbf{R}}^2. \quad (4)$$

In this equation, \mathbf{S}_ε is the measurement error covariance matrix and \mathbf{R} the regularization matrix. The diagonal elements of \mathbf{S}_ε are set to the noise level estimates, which are calculated from the fit residuals at the pre-processing step. As no spectral correlation between noise levels is assumed, the off-diagonal elements are set to zero. The regularization matrix \mathbf{R} is defined as

$$\mathbf{R} = \mathbf{S}_a^{-1} + \mathbf{T}. \quad (5)$$

Here, \mathbf{S}_a is the a priori covariance and \mathbf{T} the smoothness constraint matrices. For a particular species (in this approach NO₂ and O₃), the elements of the a priori covariance matrix \mathbf{S}_a are defined for altitudes z_i and z_j as

$$\{\mathbf{S}_a\}_{i,j} = \sigma_i \sigma_j \exp\left(-\frac{|z_i - z_j|}{I_c}\right), \quad (6)$$

where I_c is the correlation length (set to 1.5 km in this approach). σ_i and σ_j are the a priori uncertainties at the altitudes z_i and z_j , respectively. The a priori uncertainties are set to 100 % for NO₂ and 1000 % for O₃, which represents negligibly small regularization of O₃ from a priori uncertainty. With the smoothness constraint matrix \mathbf{T} (Rozanov et al., 2011), Tikhonov regularisation is applied with the smoothing parameter for NO₂ linearly decreasing with altitude from 10 at 50 km to 1.0 at 10 km, i.e. this represents stronger smoothing at high altitudes, while the constraints are weaker at lower altitudes. In the case of O₃, the smoothing parameters are set to 7.0 for all altitudes. The smoothing is done to suppress oscillations in the retrieval results while avoiding overconstraining at the same time. The Tikhonov parameters have been selected empirically to optimize the tradeoff between the sensitivity and the stability of the retrieval.

A widely used method to solve the inverse retrieval problem (see Eq. 4) is the optimal estimation with maximum a posteriori information method as described by Rodgers (2000). In this study, however, the information operator approach (Kozlov, 1983; Hoogen et al., 1999; Doicu et al., 2007) is applied instead. The idea and advantage of the information operator approach with respect to the optimal estimation method is that, in the ideal case, only those parameters are used in the fit process, which are determined by the measured information. In this approach, the solution is projected

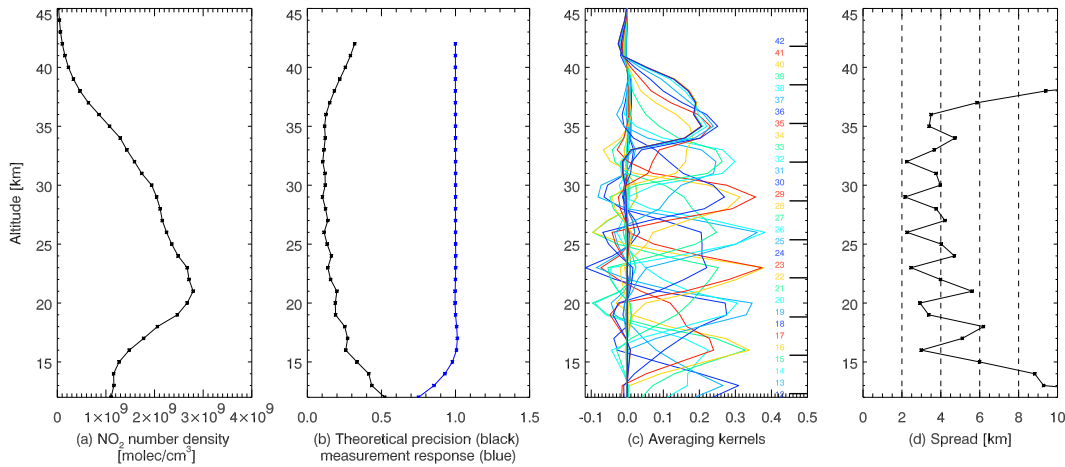


Fig. 1. An example retrieval at about 77.5° N (measurement performed on 18 June 2005) is analyzed to study the sensitivity. The retrieved NO₂ profile is shown in panel (a). Panel (b) shows the theoretical precision (black), as well as the measurement response (blue). Panel (c) displays the respective averaging kernels, color coded for altitude levels. Panel (d) shows the spread of the averaging kernels. Averaging kernels, theoretical precisions and measurement response are dimensionless quantities.

into the space of eigenvectors of the information operator, which is defined by

$$\mathbf{P} = \mathbf{R}^{-1} \mathbf{K}^T \mathbf{S}_\varepsilon^{-1} \mathbf{K}. \quad (7)$$

With the measurement, only an effective state subspace can be accessed, which is limited by considering only eigenvectors whose eigenvalues are larger than a selected threshold value. Employing the Gauss-Newton iterative approach to account for the non-linearity of the inverse problem, the solution at the $(i + 1)$ -th iterative step is written as

$$\mathbf{x}_{i+1} = \mathbf{x}_i + \sum_{k=1}^{N_i} \beta_{i,k} \boldsymbol{\psi}_{i,k}, \quad (8)$$

where $\boldsymbol{\psi}_{i,k}$ are the eigenvectors of the information operator, \mathbf{P} . The number of eigenvectors whose eigenvalues are larger than the selected threshold is represented by N_i and the expansion coefficients $\beta_{i,k}$ are given by

$$\beta_{i,k} = \frac{\eta_{i,k}}{c_{i,k}(1 + \eta_{i,k})} \boldsymbol{\psi}_{i,k}^T \mathbf{K}_i^T \mathbf{S}_\varepsilon^{-1} (\mathbf{y} - \mathbf{y}_i + \mathbf{K}_i (\mathbf{x}_i - \mathbf{x}_0)). \quad (9)$$

Here, $\eta_{i,k}$ denotes the eigenvalue of the information operator, \mathbf{P} , corresponding to the eigenvector $\boldsymbol{\psi}_{i,k}$ and $c_{i,k}$ is the following scalar product:

$$c_{i,k} = \left\langle \mathbf{K}_i^T \mathbf{S}_\varepsilon^{-1} \mathbf{K}_i \boldsymbol{\psi}_{i,k} \mid \boldsymbol{\psi}_{i,k} \right\rangle. \quad (10)$$

The iterative process is stopped when the maximum difference between the components of the solution vector at two subsequent iterative steps does not exceed 1%. Typically, three to five iterations are required to achieve the convergence.

The application of the information operator approach to the retrieval of NO₂ vertical profiles from SCIAMACHY limb measurements was previously discussed by Doicu et al. (2007).

2.2 Sensitivity of SCIATRAN NO₂ limb retrieval

The performance of the current retrieval approach is estimated by using two example retrievals. As the atmospheric properties are expected to be different at high latitudes compared with the tropics, one example measurement is selected at about 77.5° N (see Fig. 1) and the other only slightly north from the equator at 1.5° N, see Fig. 2. Both latitudes are taken from the average geolocation and ground pixel coordinates of the tangent point of the limb measurement. Due to the strong diurnal and seasonal variation, generalizations of these results for the tropics and the high latitudes should be avoided.

It should be noted that in the tropics example, the retrieved NO₂ maximum is found at an altitude of about 33 km with 1.4×10^9 molec cm⁻³, and at the high latitudes example, it is about 2.8×10^9 molec cm⁻³ at about 21 km altitude.

To illuminate the analysis as displayed in the Figs. 1 and 2, each feature is explained in detail. The theoretical precisions describe the total retrieval error (noise + smoothing errors) and are calculated from the square root of the diagonal elements of the solution covariance matrix $\hat{\mathbf{S}}$ (see Rodgers, 2000). $\hat{\mathbf{S}}$ corresponds to the result of the last iteration in the retrieval process $\hat{\mathbf{x}}$ and is defined as

$$\hat{\mathbf{S}} = \left(\hat{\mathbf{K}}^T \mathbf{S}_\varepsilon^{-1} \hat{\mathbf{K}} + \mathbf{R} \right)^{-1}. \quad (11)$$

For the tropics example, the precisions are similar above 18 km and poorer at lower altitudes than at the high latitudes example, which is related to much lower NO₂ concentrations at lower altitudes in tropics.

The measurement response given in the same panels is calculated by summing up the area below the averaging kernels. It describes the degree of which the measurements contribute

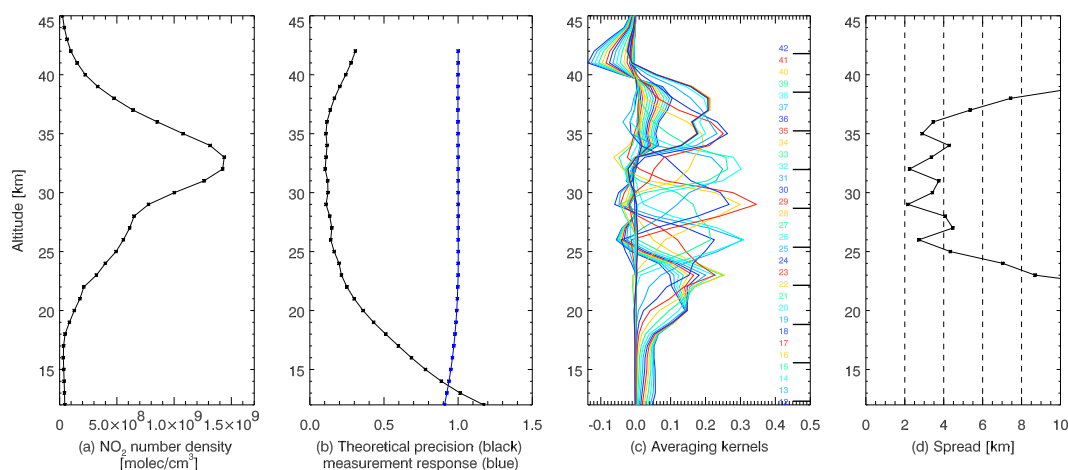


Fig. 2. Similar to Fig. 2, a retrieved NO₂ profile is analyzed. However, this example (measurement performed on 18 June 2005) is obtained at 1.45° N. Panel (a) shows the NO₂ profile retrieved with SCIATRAN, panel (b) theoretical precision (black) and measurement response (blue), panel (c) averaging kernels and panel (d) spread.

to the retrieved profile. Values close to 1 indicate that the retrieved profiles are mostly unbiased by a priori information.

Comparing the two examples, the response function is generally close to 1 and starts to decrease below 20 km in the tropics and 15 km in the high latitudes, i.e. the lowest altitude unbiased by a priori is lower for the high latitudes example. A decrease of the measurement response below 15 km is caused by the cut off of the averaging kernels at 12 km. Because of larger averaging kernels this has a stronger effect at high latitudes.

The averaging kernels are presented in panel c. As they are calculated on a 1 km grid compared to the resolution of about 3.3 km of the instrument, highest expected values are between 0.3 and 0.4. At about 43 km, averaging kernels are expected to be negative as this is the reference tangent height used for retrieval. This is best seen in Fig. 2. The vertical resolution of the retrieval can be estimated from the width of the averaging kernels which, however, is difficult to quantify. The Backus and Gilbert approach (Backus and Gilbert, 1970, used e.g. in Haley et al., 2004) helps with the definition of a characteristic called spread, calculated with

$$s(z) = 12 \frac{\int (z - z')^2 \mathbf{A}^2(z, z') dz'}{\left[\int |\mathbf{A}(z, z')| dz' \right]^2}. \quad (12)$$

The altitude is given as z and \mathbf{A} denotes the averaging kernel matrix. As expected, the spread profiles show the best vertical resolution near the averaging kernel maxima. The measurement tangent heights are located about 1 km below these minima. For example, the tangent heights for Fig. 1 in the altitude range from 20 to 30 km are given for 21.80, 25.05, and 28.35 km, while the spread minima are at 23.0, 26.0, and 29 km.

In the tropics example (Fig. 2), the spread shows favorable values between 37 and 25 km with values between 2 and less

than 6 km. At the high latitudes example, this range covers 37 to 15 km. Below 15 km (25 km in the tropics example), the low signals resulting from a combination of small NO₂ values and an increasing optical path along the line-of-sight lead to a reduced vertical resolution.

Although these are arbitrary examples, the NO₂ maximum is seen at higher altitudes closer to the equator. In most cases, the altitude range, for which SCIAMACHY is sensitive to NO₂, matches the respective altitudes ranges covered by the occultation instruments used for validation in a reasonable way.

2.3 Photochemical correction of NO₂

NO₂ is a photochemically active species and has a pronounced diurnal variation. This causes difficulties for validation efforts, as two measurements performed at different local times cannot be compared directly. For the validation of NO₂ vertical profiles, one of these two profiles has to be photochemically corrected to match the illumination conditions of the other measurement.

To perform this correction, the photochemical box model developed at the University of California, Irvine (Prather, 1992; McLinden et al., 2000) is used to create look-up tables. For three days in a month (1st, 11th and 21st day), on a latitude grid of 2.5° and for an altitude range from 8 to 56 km (step size 2 km, pressure altitudes), complete diurnal circles of NO₂ are modelled.

From the NO₂ profiles at the geolocations and times of both measurements, scaling factors can be calculated. When using the look-up tables for photochemical correction, the latitude closest to the location of the SCIAMACHY measurements is selected from the table. As SCIAMACHY measures near the local noon, i.e. at high solar elevation, there might be a situation where the SZA of SCIAMACHY is not reached

at the closest tabulated latitude. Such collocation pairs are rejected from the comparison. After applying the collocation criteria described later in Sect. 3.1, less than 10 % collocations are discarded at this step. For ACE-FTS, this is seen more often, which can be explained with a different orbit resulting in a relatively large amount of measurements at high latitudes, where the aforementioned issue occurs.

The scaling factors are then applied to NO₂ profiles from the occultation instruments (ACE-FTS, SAGE II or HALOE) and the photochemically corrected NO₂ profiles are compared with the matching SCIAMACHY NO₂ profiles.

As discussed by Bracher et al. (2005), the uncertainty of the photochemical correction is estimated to be about 20 %. In this work, however, a look-up-table is used for photochemical corrections instead of full model runs, which might introduce an additional error source. The difference between using full model runs (with pressure and temperature information for the time and location of the SCIAMACHY measurements from the ECMWF database and ozone profiles from the same SCIAMACHY measurements) and the look-up-table from the same model is estimated to be less than 10 % above 20 km and can exceed 50 % below this altitude.

2.4 Error discussion

NO₂ retrieval results are influenced by an array of different error sources, and it is important to quantify these in order to decide whether a difference between SCIAMACHY and other instruments is within expectations or not. Generally, retrieval errors contain the smoothing error, the model parameter error, the forward model error and the retrieval noise. Of these errors, the smoothing error is of less importance, as it originates from the finite resolution of the instrument with respect to the true state. We do not know the true state and perform comparisons with measurements from real instruments instead, which are also always subject to smoothing errors depending on their resolution. The NO₂ products discussed here show reasonably similar vertical resolutions in the range of 2 to 4 km (see Sect. 3.2).

For each SCIAMACHY NO₂ limb profile, theoretical precisions are provided, as described in Sect. 2.2. They are below 10 % for altitudes between 25 km and 35 km and below 15 % for altitudes between 22 and 42 km (tropics) or 16 and 42 km (high latitudes).

Errors in the temperature and pressure profiles have an insignificant influence on SCIAMACHY NO₂ retrieval results in limb mode (less than 5 %) above 20 km as discussed in Rozanov et al. (2005), as accurate ECMWF data are used in the retrieval process.

The influence of aerosols on NO₂ limb retrieval results for SCIAMACHY is estimated by using synthetic retrievals. The retrieval examples shown in Figs. 1 and 2 are used for a forward simulation perturbed with two volcanic scenarios for the stratosphere from LOWTRAN (Kneizys et al., 1988, namely, aged aerosols from moderate volcanic activity and

fresh aerosols from high volcanic activity), and with a scenario with no aerosols in the forward model, all seen in Fig. 3. Above 22 to 25 km, the influence of aerosols is small (less or about 5 %) for all investigated scenarios and is considered larger below this altitude. For the tropical scenario, the relative errors at low altitudes need to be interpreted carefully, as very low NO₂ values have high relative errors. Because of a low volcanic activity during the time period considered in this paper, the typical influence of the stratospheric aerosol on the retrieval results is expected to be low.

Pointing errors (i.e. uncertainties in the tangent point altitudes given for the measurements of SCIAMACHY) are estimated to be below 200 m in SCIAMACHY Level 1 data version 6.03 (von Savigny et al., 2009). It is worth mentioning that version 6.03 introduced improvements in pointing accuracy with respect to previous versions, as discussed by von Savigny et al. (2007). Simulations were done shifting the measurement tangent heights by ± 200 m. Then, the retrievals were made assuming no pointing shift, see Fig. 4. For the high latitudes, the relative deviation of the perturbed scenario with respect to the scenario without a change in altitude does not exceed 5 %. In the tropics, the relative difference is below 12 % above 22 km and exceeds 50 % at 15 km, as the NO₂ concentrations are very small at these altitudes.

To estimate the influence of cloud contamination on NO₂ profiles, a series of synthetic retrievals is performed for both water and ice clouds at different altitudes and SZAs with different geometrical and optical thickness. The clouds were simulated in the SCIATRAN forward model. Figure 5 shows the influence of the water clouds with different geometrical and optical thickness on the retrieval results at a SZA of 35°. This is a tropics example, and the synthetic profiles show relative differences of less than 6 % above 25 km between the unperturbed case and the profiles perturbed by water clouds with different parameter settings. The results for ice clouds are almost identical for this SZA and, hence, not shown here. The maximum relative difference of about 6 % above 17 km is found for a SZA of 70° for both water (Fig. 6) and ice clouds (Fig. 7). It should be noted that a cloud with a top altitude of 15 km is not very likely to be found at high latitudes. For the investigation at lower altitudes or to avoid clouds of higher altitudes (PSCs, NLCs), the SCIAMACHY NO₂ product includes results from the cloud detection algorithm SCODA, as mentioned in Sect. 2.1. We applied this method for cloud masking on the results in this paper for testing purposes. However, while about two thirds of all collocations are sorted out, the results do not show any significant difference or improvement in the selected altitude range. In the sensitivity studies, clouds are not a large error source above 20 km. Below this altitude, other error sources are also significant. Therefore, it was decided not to apply cloud masking and to keep the higher number of collocated profiles.

The diurnal variation of NO₂ also affects the retrieval results directly. This problem is not solved with the photochemical corrections applied here and will be referred to as

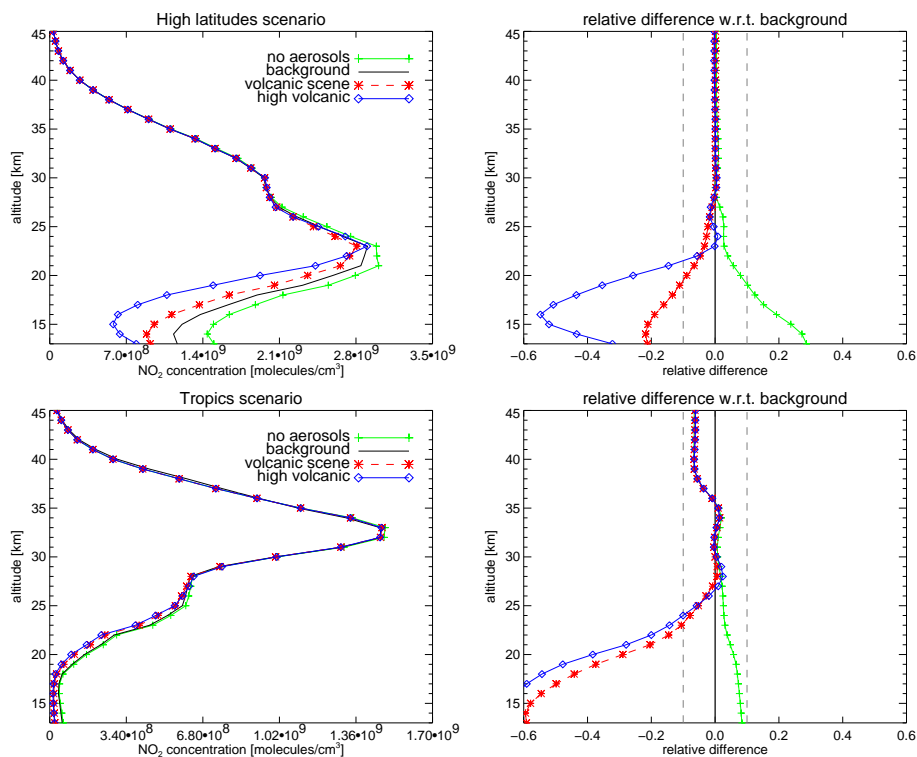


Fig. 3. Influence of the stratospheric aerosols on the retrieved NO₂ profiles. Left panels show NO₂ profiles retrieved for different aerosol loadings at northern high latitudes (upper panels) and in the tropics (lower panels), 18 June 2005. Right panels show corresponding relative deviations.

the diurnal effect error (see McLinden et al., 2006). It is related to the changing SZA along the line of sight for a limb or occultation measurement that is not accounted for in the retrieval. The high gradient of NO₂ during sunrise and sunset introduces significant errors. This error has a similar order of magnitude at high SZAs close to 90°, which is the case for polar latitudes, for SCIAMACHY NO₂ as for occultation instruments. In the tropics and mid latitudes, this error is expected to be small for SCIAMACHY, since the measurements are made at smaller SZAs resulting in a much less rapid change in NO₂ along line of sight. When estimating the influence of the diurnal effect on the comparison results in this study, we always assume the effect to be small for SCIAMACHY retrievals, which is strictly true only for a range of SZAs, which are not too large.

Precalculated synthetic retrievals from occultation instruments on a 2.5°-latitude grid with the diurnal effect error considered in the forward model $\mathbf{x}_{\text{sim}_w}$ and without the diurnal effect error in the forward model \mathbf{x}_{sim} are used to estimate the diurnal effect error for individual occultation measurements:

$$\epsilon_{\text{diurnal}} = \frac{\mathbf{x}_{\text{sim}_w} - \mathbf{x}_{\text{sim}}}{\mathbf{x}_{\text{sim}}}. \quad (13)$$

The results from these calculations are discussed in Sect. 3.3.

3 Validation of NO₂

All NO₂ data products used for validation of SCIAMACHY results in this work are retrieved from solar occultation measurements. While HALOE and SAGE II ceased operations in 2005, the newer instrument ACE-FTS continues to deliver measurements as of 2011. If available, number densities are taken directly from the data sets (SAGE II). Otherwise, they are calculated from volume mixing ratios using the pressure and temperature profiles provided in the respective data sets (HALOE, ACE-FTS).

3.1 Collocation criteria for validation

Allowed pairs of measurements for validation were chosen to have a maximum spatial difference of 500 km and a maximum time difference of 8 h. In addition, tropopause heights at geolocations of both measurements are required to differ not more than 2 km, unless both are below 10 km. The tropopause heights are calculated from ECMWF pressure and temperature profiles using the method from Hoinka (1998) and provided at a 1.5° × 1.5° grid (F. Ebojje, personal communication, 2010), from which the nearest neighbor is selected. To avoid comparisons of profiles at different vortex conditions, the potential vorticity at the isentropic level of 475 K is analyzed in a similar way as described by Bracher

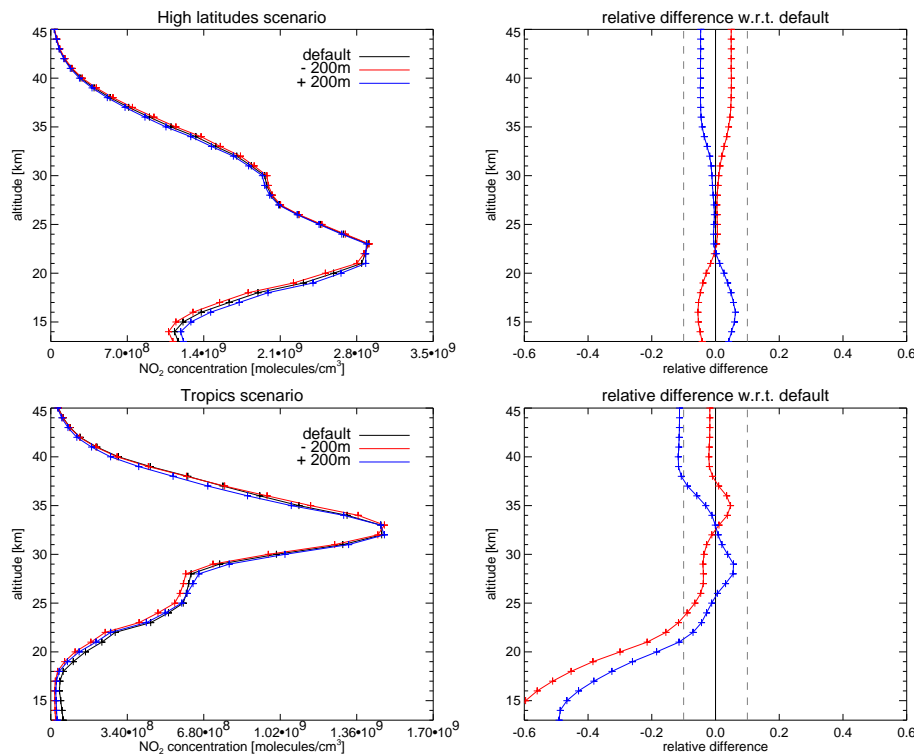


Fig. 4. Influence of the pointing errors on the retrieval results for northern high latitudes (upper panels) and tropics (lower panels), 18 June 2005. Left panels show the retrieved profiles for shifted ± 200 m and unperturbed tangent heights. Right panels show the corresponding relative deviations.

et al. (2004). The potential vorticities are calculated from the UKMO (United Kingdom Meteorological Office) assimilated meteorological data set (with a grid of $3.75^\circ \times 2.5^\circ$) with the method described by Sonkaew (2010). The collocations are used for validation if the potential vorticity for both measurements is similar, i.e. either below -40 PVU, or above 40 PVU or in the range from -30 to 30 PVU. These criteria are applied automatically, which allows numerous comparisons.

3.2 Satellite instruments used for validation

The Stratospheric Aerosol Gas Experiment (SAGE II) instrument (Chu et al., 1989) flew on board the Earth Radiation Budget Satellite (ERBS) launched in 1984. As the ERBS had a very long operational time (21 yr), there is a long overlap of several years with SCIAMACHY from 2002 to 2005. With SAGE II, aerosols, ozone, NO₂, and water vapour were measured. For SAGE II NO₂, the vertical resolution is about 2 km (Gordley et al., 1996), the field of view of the instrument is 0.5 km. SAGE II Version 6.2 data products are used in this study.

Errors for SAGE II reported in the datasets are between 10 % and 5 % for altitudes from 25 km to 35 km for most measurements. Below 25 km errors reach values of about 50 %, and exceed 10 % above 35 km. These values include

altitude uncertainty, temperature profile errors which affect the removal of the Rayleigh-scattered contributions, errors from the removal of ozone and aerosol contributions, and measurement errors (see Cunnold et al., 1991).

Launched on 12 September 1991, the UARS satellite (Upper Atmosphere Research Satellite) carried several instruments for the investigation of the Earth's atmosphere. One of its ten instruments was the Halogen Occultation Experiment (HALOE, Russell III et al., 1993; Russel III and Remsburg, 2012). HALOE was intended to perform solar occultation measurements of ozone (O₃), hydrogen chloride (HCl), hydrogen fluoride (HF), methane (CH₄), water vapour (H₂O), NO, NO₂ (Gordley et al., 1996) and aerosol extinction at 4 infrared wavelengths. Additionally, pressure and temperature profiles were also retrieved. The satellite has been deactivated in December 2005.

In this study, HALOE Version 19 data, which have been screened for cirrus clouds, are used for validation (Hervig and McHugh, 1999). A correction for the diurnal effect error is also applied. The vertical resolution of NO₂ data is 2 km. The dataset includes random noise error plus aerosol induced error as uncertainties, as discussed in Gordley et al. (1996), along with an estimated total error not including aerosol related errors. For HALOE, this total error is smaller than 10 %

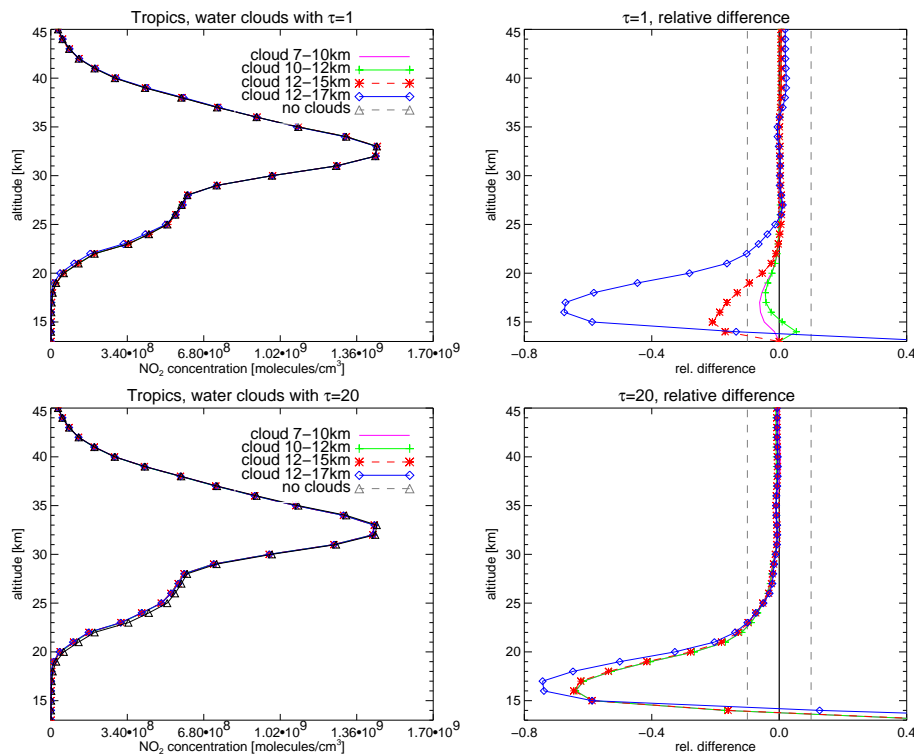


Fig. 5. Influence of water clouds with an optical thickness of 1 (upper panels) and 20 (lower panels) on the retrieved results at the tropics example (SZA = 35°), 18 June 2005. Left panels show the NO₂ profiles retrieved for different clouds. Right panels show corresponding relative deviations.

between 25 km and 35 km, smaller than 20 % between 35 and 40 km, and larger than 40 % below 20 km.

One of the instruments of SCISAT-1, a Canadian satellite launched in August 2003, is ACE-FTS (Atmospheric Chemistry Experiment-Fourier Transform Spectrometer, Walker et al., 2005; Bernath et al., 2005). Still operational as of 2012, ACE-FTS allows a validation of more recent results compared to SAGE II and HALOE. Including NO₂ and O₃, the ACE-FTS instrument is able to perform measurements of a large variety of atmospheric species. The vertical resolution of the measurements is 3 to 4 km based on the field of view of ACE-FTS (1.25 mrad).

In this study, ACE-FTS Level 2 version 2.2 data products are used, see Boone et al. (2005) for the retrieval method. The uncertainties given are the statistical fitting errors from the least-squares process with a normal distribution of errors assumed (Kerzenmacher et al., 2008). These errors are given as less than 5 % in the altitude range used for analysis (20 to 40 km), while the errors are higher than 10 % below 20 km and exceed 40 % at 15 km.

However, because of the different calculation methods and included error sources, the uncertainty values are not easily comparable.

3.3 Validation results

The validation results are shown as scatter plots (for SCIAMACHY profiles and the respective photochemically corrected profile) for three different altitude regions, given as partial vertical NO₂ columns (20 to 25 km, 28 to 32 km and 35 to 40 km). This means, that the NO₂ amounts are summed up in 1 km steps for each altitude range. In each scatter plot, results from different latitude regions are identified by color. To avoid bias resulting from seasonal differences in NO₂ amounts, collocations from each season are analyzed separately. For example, the panels marked with D, J, F (December, January, February) contain collocations from the meteorological winter in the Northern Hemisphere and meteorological summer in the Southern Hemisphere. Linear regression parameters are also given (three cases: all/sunset/sunrise collocations) and the linear regression curve is plotted for all collocations in the scatter plot. However, these parameters can still be influenced by seasonal variations, as northern and southern seasons are mixed in the calculation.

For further investigation, at each altitude h the relative difference RD can be calculated for each collocation pair, defined as:

$$RD(h) = \frac{x_{SCIA}(h) - x_{Val}(h)}{(\overline{x_{SCIA}}(h) + \overline{x_{Val}}(h)) \times 0.5}, \quad (14)$$

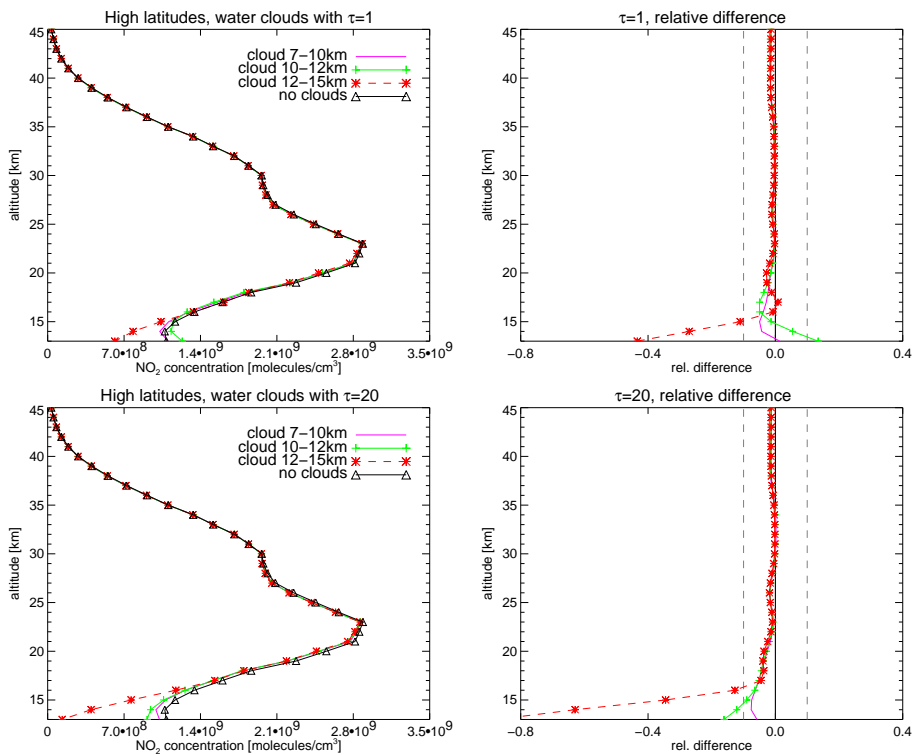


Fig. 6. Same as Fig. 5, but for northern high latitudes (SZA = 70°), same day.

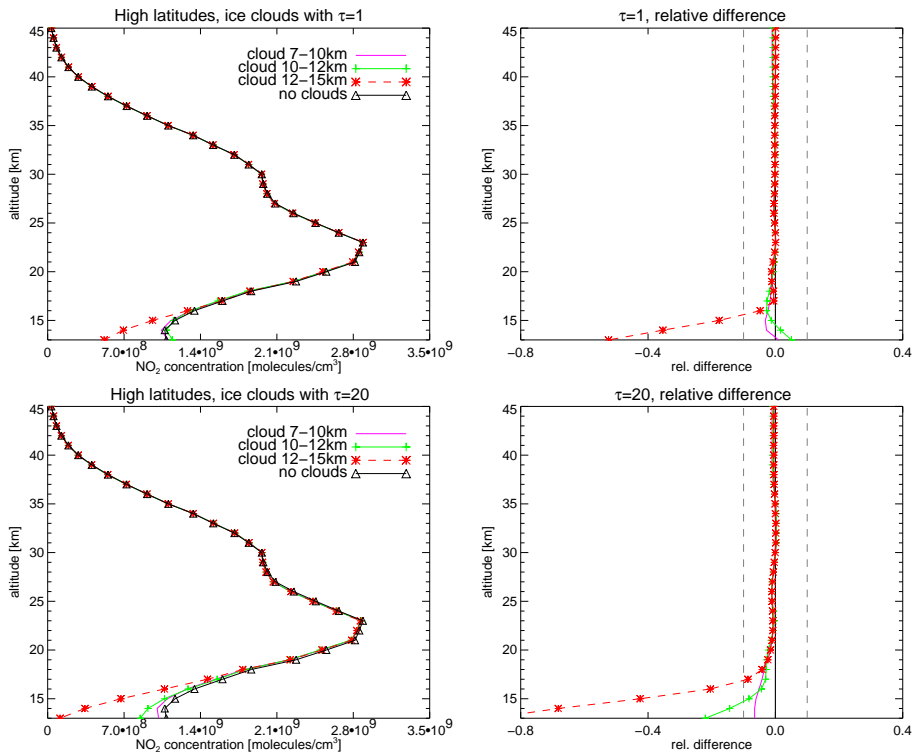


Fig. 7. Same as Fig. 6, but for ice clouds.

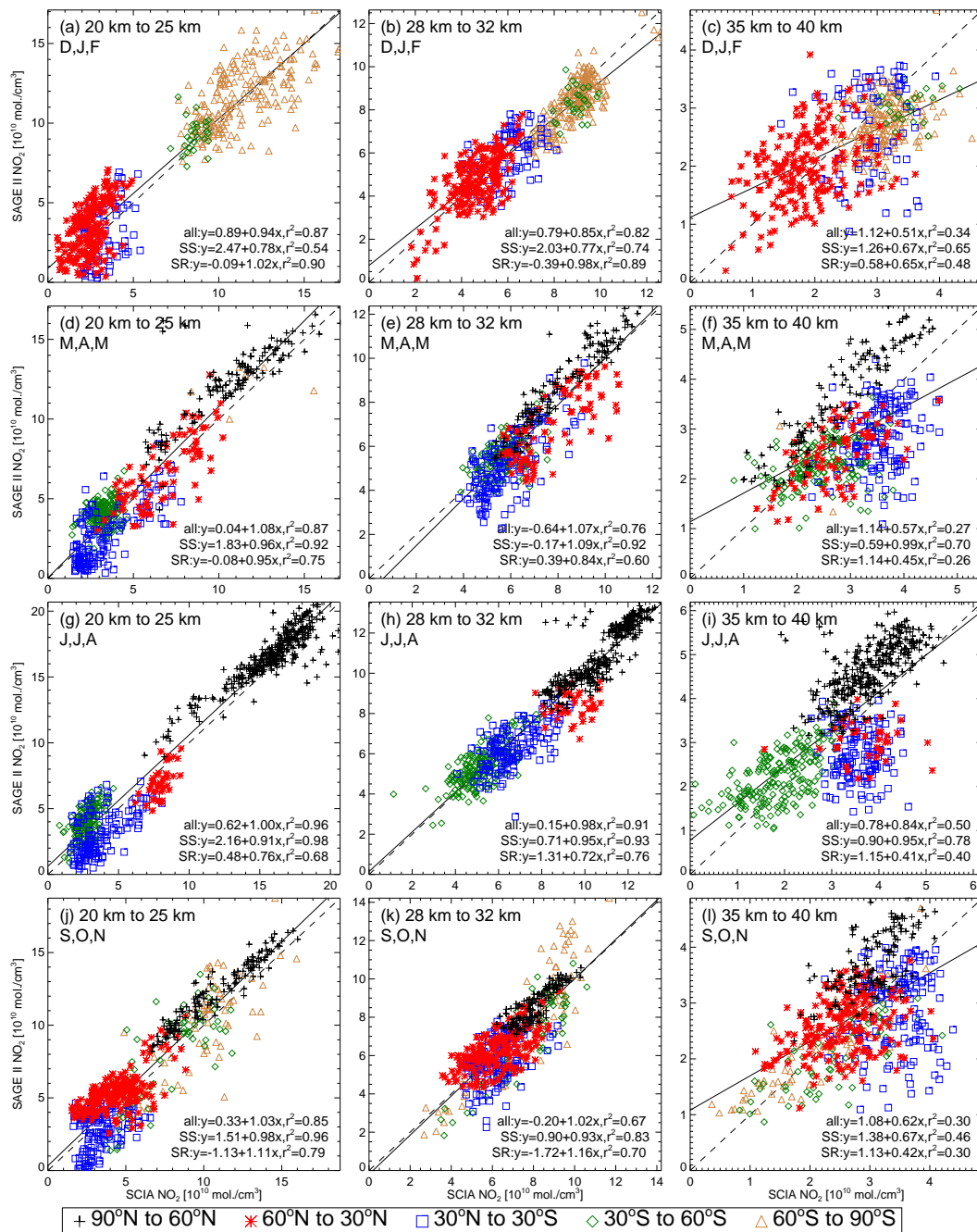


Fig. 8. Scatter plots of collocated SCIAMACHY and photochemically corrected SAGE II NO₂ results for the years 2003 and 2004 are given for partial vertical columns and grouped in 4 seasonal and 3 altitude ranges (20 to 25 km, 28 to 32 km, and 35 to 40 km). 2338 collocation pairs are shown (1121 for SAGE II sunset and 1217 for sunrise). In each panel, collocated pairs from different latitude regions are shown with different colors as given in the legend above.

with x_{SCIA} as SCIAMACHY NO₂ number densities and x_{Val} as number densities from the respective validation source. The profiles are normalized with respect to the average of the mean SCIAMACHY NO₂ profile $\overline{x_{\text{SCIA}}}$ and the mean profile from the validation source $\overline{x_{\text{Val}}}$. Both mean NO₂ are calculated from the respective collocation subset. This definition

avoids the problem of overemphasized relative deviations due to occasionally very small NO₂ amounts.

In Fig. 8, a comparison for the profiles in 2003 and 2004 is given for SAGE II and SCIAMACHY with 2338 comparisons, after all collocation criteria are applied as mentioned in Sect. 3.1. Of these 2338 cases, 1121 SAGE II measurements

were performed during sunset and 1217 during sunrise. The panels on the lefthand side represent partial vertical columns from 20 to 25 km, the middle columns from 28 to 32 km and the panels on the righthand side from 35 to 40 km. The upper panels include collocations from the months December, January and February (winter in the Northern Hemisphere and summer in the Southern Hemisphere), the panels d to f the months March, April and May, panels g through i the months June, July and August, while the lowermost panels j to l contain collocation pairs from September, October and November. In each panel, latitudinal regions are color-coded, i.e. black for 90° N to 60° N, red for 60° N to 30° N, blue for 30° N to 30° S, green for 30° S to 60° S, and brown for 60° S to 90° S.

It should be noted, that due to the orbits of the satellite instruments, collocations might not be found for some seasons and latitude bins, as listed in Table 1. For example, in NH winter season (December, January and February) no collocations in the 90° N to 60° N latitude range are found for SAGE II, see also panels a to c of Fig. 8.

While for lower altitudes (20 to 25 km and 28 to 32 km) the squared correlation coefficient r^2 is larger than 0.80 in most cases and the slope is mostly close to 1, this is not the case for the 35 to 40 km altitude range. At these altitude levels, NO₂ amounts are generally small. Because of the small dynamic range, the linear regression parameters have larger uncertainties.

For sunset measurements, r^2 is higher than for sunrise measurements with the notable exception of the uppermost panels, which include a large number of SAGE II sunrise measurements in the SH summer. Thus, the linear regression curve given in each panel is not only influenced by using measurements from different regions, but also by the relative amount of sunset/sunrise measurements as well. Generally, the quality of SAGE II NO₂ results is lower for sunrise measurements as a result of technical issues (see Cunnold et al., 1991). This is also seen in a comparison with ACE-FTS (Kerzenmacher et al., 2008), which agrees well with sunset SAGE II NO₂, but has a significant high bias compared to sunrise SAGE II NO₂ amounts. This high bias is, however, not seen when comparing ACE-FTS to the other satellite instruments in the analysis.

To discuss the results of the scatter plots, average NO₂ profiles are calculated and shown in Fig. 9. Averaged SCIAMACHY NO₂ amounts for each bin are shown in black, and standard deviations of these values calculated for the particular collocation sample are given as black dashed lines. Photochemically corrected and averaged SAGE II NO₂ amounts are plotted as red line, and the respective standard deviations are shown as red-dashed line. As expected for SCIAMACHY measurement conditions, the NO₂ levels are largest in summer conditions at high latitudes. In NH summer (JJA) conditions, NO₂ levels decrease southwards with the lowest values seen in the 30° S to 60° S latitude range. Unfortunately, there are no collocations available south of 54.3° S, see Table 1.

Table 1. Latitude ranges for all collocations with SCIAMACHY for each season and instrument in the years 2003 and 2004 (2004 and 2005 for ACE-FTS).

Months	SAGE II	HALOE	ACE-FTS
DJF	56.6° N–78.0° S	56.0° N–73.2° S	80.0° N–68.4° S
MAM	80.3° N–79.5° S	78.0° N–74.9° S	83.4° N–78.8° S
JJA	78.0° N–54.3° S	72.5° N–54.7° S	68.2° N–63.6° S
SON	78.1° N–68.6° S	77.8° N–78.7° S	83.7° N–76.0° S

This is mirrored in NH winter conditions (DJF), with the largest NO₂ amounts in the South (30° S to 60° S). In the Tropics (30° N to 30° S), NO₂ levels are low on average, especially at altitudes below 25 km. This directly influences the validation results, as high NO₂ levels are expected to be easier detected. Also, the same absolute NO₂ errors result in large relative differences, if the NO₂ levels are small.

From the relative differences (RD) calculated with Eq. (14), mean values (MRD) are computed for each latitude/season bin and summarized in Table 2. The MRD values are given for an altitude range from 20 to 40 km for sunset and sunrise values separately. The MRD_{corr} values are related to the diurnal effect error correction and are discussed later. In the same table, SZAs and average local times \bar{t} for the SCIAMACHY measurements and the number of collocations, n (sunset/sunrise), are given. The MRD is not calculated for cases with less than 10 collocations. Since SCIAMACHY measurements at NH high latitudes can include afternoon measurements, these local times are averaged separately. Large relative NO₂ differences can be found in tropics, while small MRDs are correlated with higher NO₂ amounts. Because of the increasing difference in SZA, the uncertainty of the photochemical correction increases from high latitudes to tropics. It is noteworthy, that between 90° N to 60° N, SAGE II NO₂ levels are generally higher than SCIAMACHY. Since all measurements at 90° N to 60° N in this comparison are sunset measurements, this agrees well with Bracher et al. (2005). Similar results were also reported for the comparison of data from MIPAS (Michelson Interferometer for Passive Atmospheric Sounding) instrument on ENVISAT with SAGE II results (see Wetzel et al., 2007). At 76° N to 60° N and pressure levels from 32 to 2.7 hPa, mean relative differences (normalized w.r.t. to SAGE II) were found to be within –32 to –11 % for several months from April to September in 2002 and 2003. This agrees well with the present results at similar regions and timeframes (e.g. –36 % to –8 % at 90° N to 60° N in June to August – J, J, A). While the results for other latitude ranges agree less well, the tendency for more positive MRDs at southern latitudes is present as well (e.g. 63° S to 80° S in December and February, 27 to 2.3 hPa, 0 to 38 % compared with –10 to 6 % in the present work). Unfortunately, the distribution of the coincidences between SAGE II sunset and

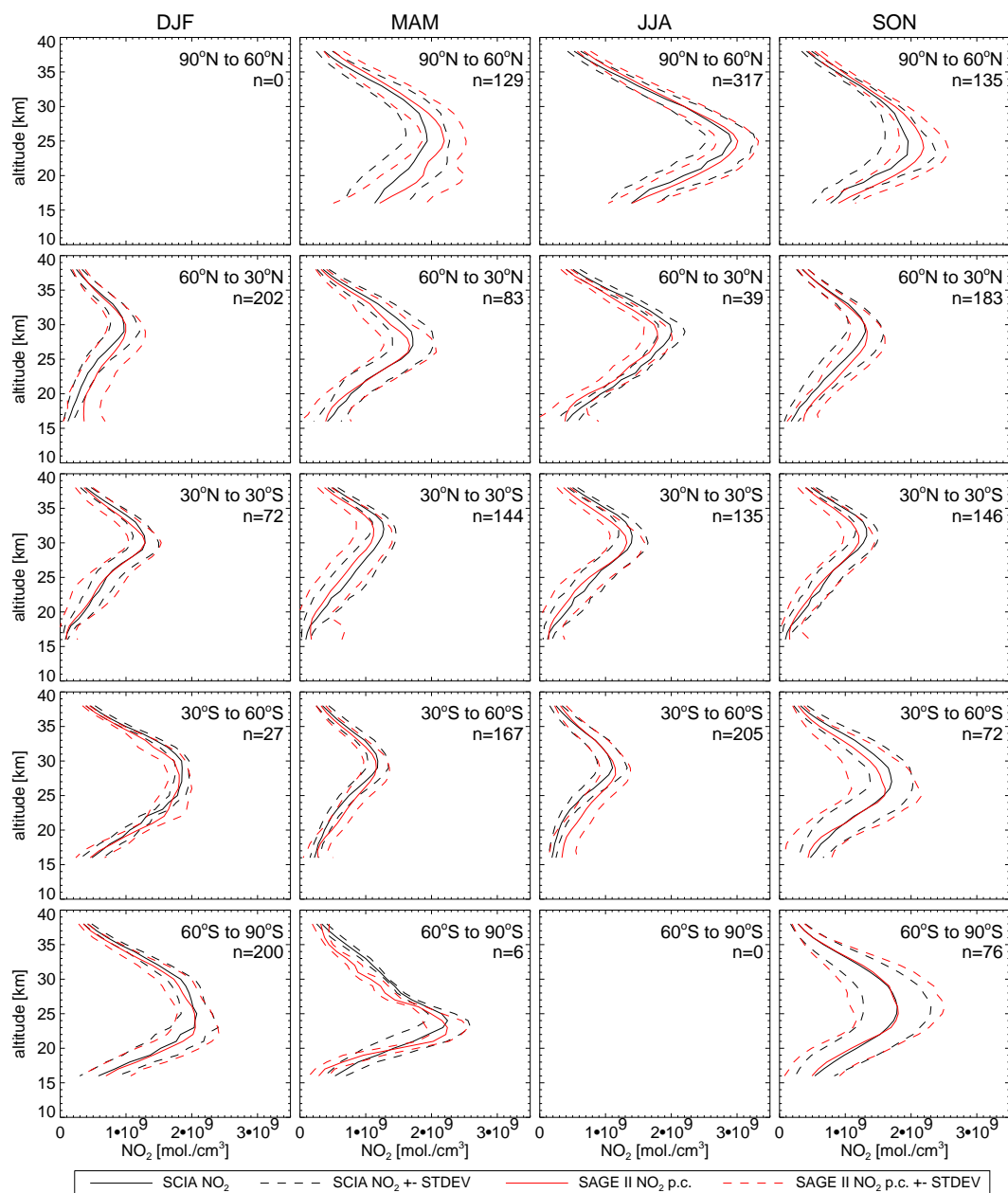


Fig. 9. From the SCIAMACHY and SAGE II collocation pairs for 2003 and 2004, vertical NO₂ profiles are averaged for collocation subsets of different latitude ranges and seasons. The panels are ordered from top to bottom depending on latitude range, with northern latitudes on top. The panels are also ordered from left to right depending on season. In each panel, the NO₂ profiles are averaged for SCIAMACHY (black line) and photochemically corrected SAGE II NO₂ profiles (red). The standard deviations for both subsets are given as dashed lines in the respective color and added/subtracted from the averaged profiles.

sunrise measurements was not discussed, which might have an impact on the mean relative differences.

An important error source in the compared data is the diurnal effect error. NO₂ concentrations from solar occultation instruments show a significant high bias at altitudes below 25 km if the diurnal effect error is not considered. Since it is known to vary depending on latitude and season (Brohede et al., 2007), an individual error estimation is calculated for

each collocation pair. For profiles and latitude zones (except for high latitudes) shown in Fig. 9, the mean values for the relative diurnal effect error are presented in panels a to d of Fig. 10.

To estimate the influence of the diurnal effect error on retrieved NO₂ profiles, each photochemically corrected SAGE II NO₂ profile is adjusted with the matching estimated diurnal effect error. As sunset and sunrise measurements are

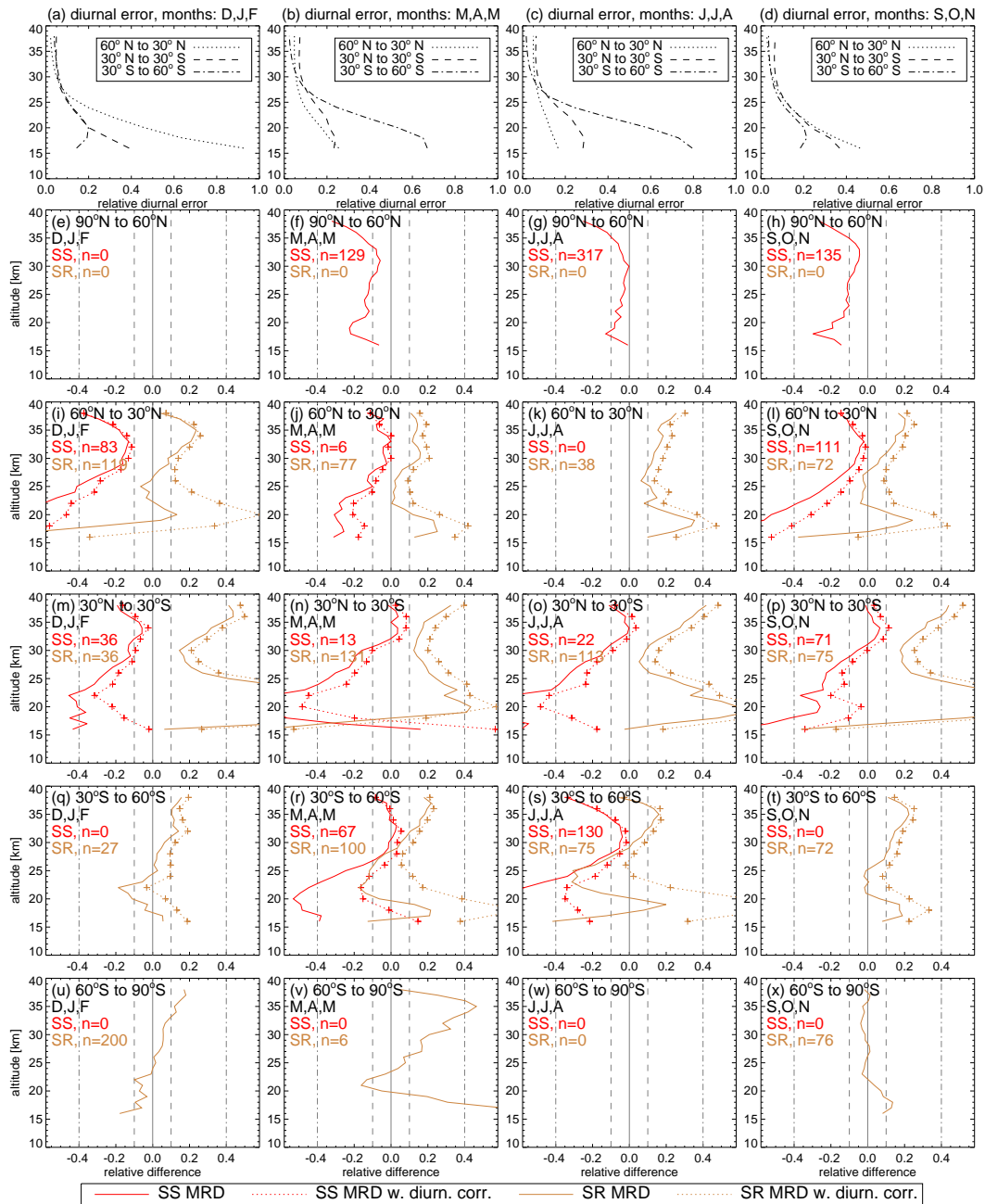


Fig. 10. Panels (a) to (d): relative diurnal effect errors for the SAGE II profiles shown in Fig. 9. A model was used to estimate the diurnal effect error for each SAGE II occultation. These represent the mean errors over the latitude/seasonal bin. The influence of this error on the agreement between the SAGE II and SCIAMACHY is estimated in panels (i) to (t) for each latitude and season. MRDs with photochemical corrections and without diurnal effect error correction are displayed as red (sunset) and orange (sunrise) solid lines. MRDs with consideration of the diurnal effect error are given as dashed lines with the same color-coding.

expected to lead to different results, the correction is applied separately for these cases. The red curve in panels e to x shows averaged RDs calculated with Eq. (14) for SAGE II sunset conditions while sunrise conditions are shown in orange. In both cases, a dotted line gives the mean relative differences MRD_{CORR} after the diurnal effect error correction

has been applied. The MRD_{CORR} values are summarized in Table 2.

This is not done for high latitudes, as the SCIAMACHY profiles with high SZAs are also expected to be significantly influenced by the diurnal effect error. Although the agreement is improved for sunset measurements, the relative

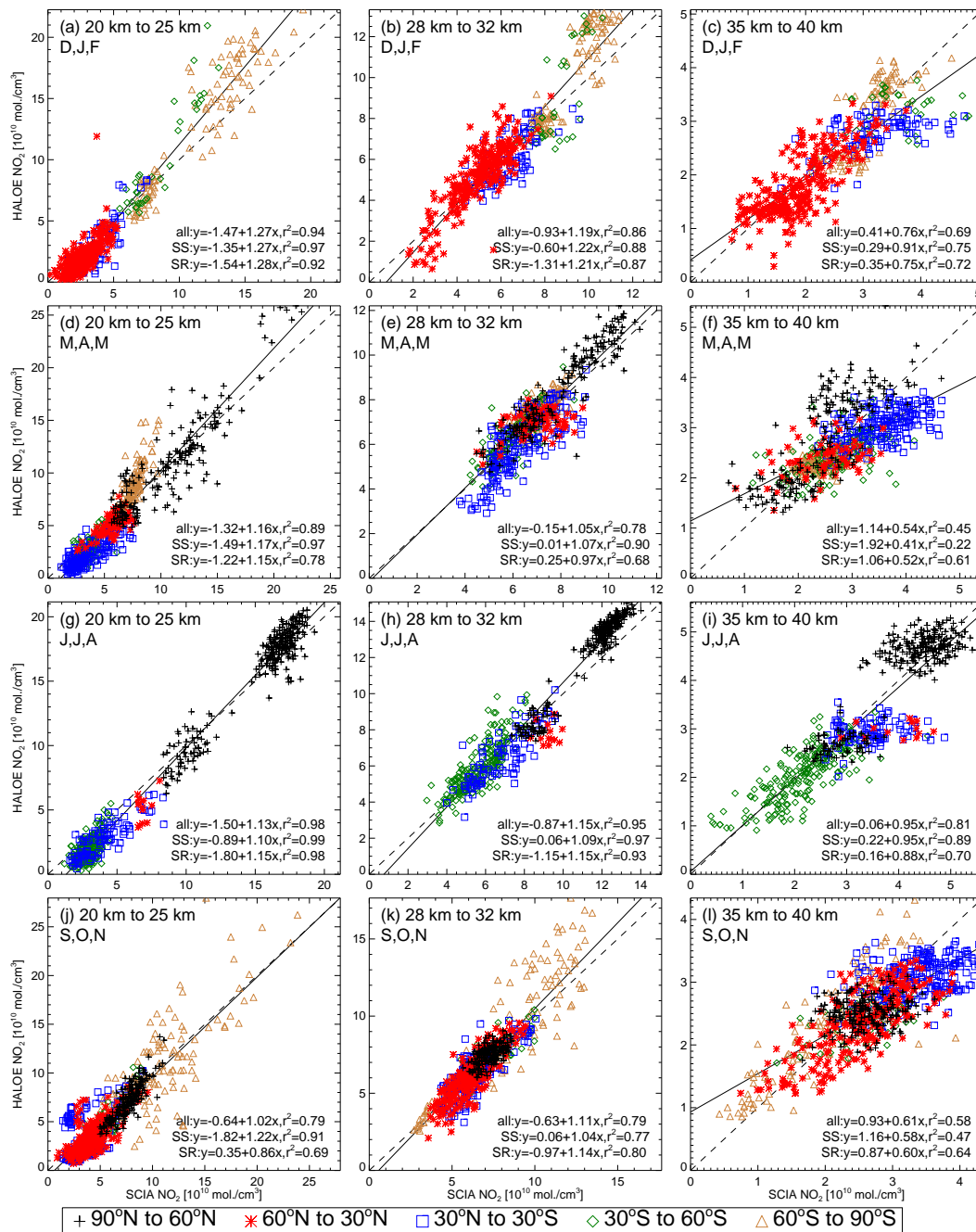


Fig. 11. Same as Fig. 8, but for HALOE data. 2592 collocation pairs are shown (913 for HALOE sunset and 1679 for sunrise).

differences increase for sunrise measurements. As discussed before, there is a significant difference between SAGE II NO₂ sunset and sunrise NO₂ comparisons with sunset measurements believed to be of a better quality, which is a known feature of SAGE II.

Similarly to SAGE II, available data allow a comparison of the years 2003 and 2004 for HALOE with a total of 2592 comparisons. As for SAGE II, the comparison results are presented as a scatter plot, see Fig. 11. In comparison,

the r^2 levels are mostly closer to 1, and the differences between sunset and sunrise linear regression parameters are smaller. For 20 to 25 km and 28 to 32 km, the SCIAMACHY NO₂ amounts are smaller on average compared with HALOE NO₂.

Figure 12 shows the average vertical distributions from SCIAMACHY and HALOE in a similar way as it was done for SAGE II (see Fig. 9). Again, the MRD values in Table 3 are smaller for latitude/season bins with generally larger NO₂

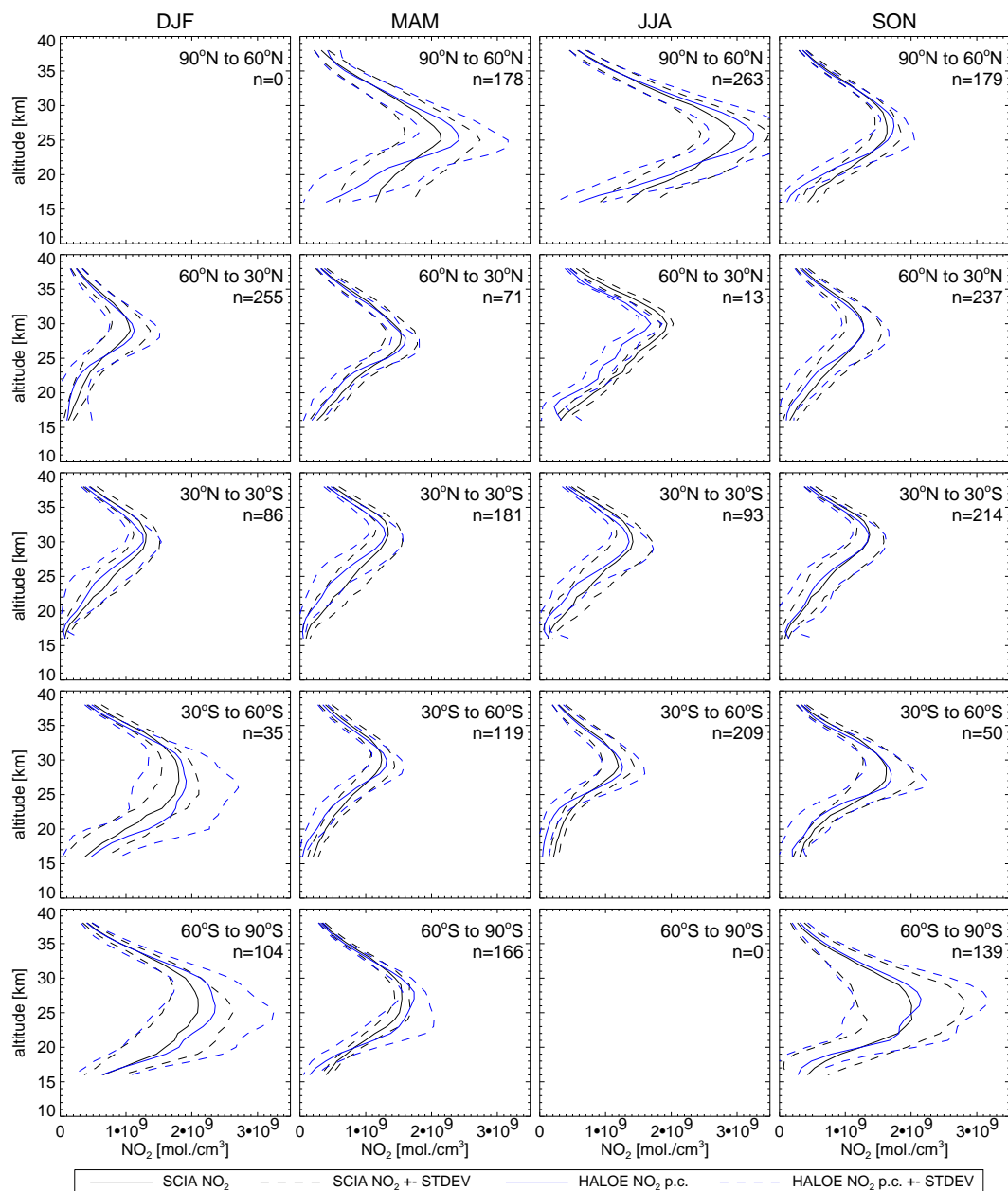


Fig. 12. Same as Fig. 9, but for HALOE data.

amounts. Contrary to SAGE II, it is the SCIAMACHY product which shows larger NO₂ amounts than HALOE, at least for altitudes below 20 km, which are not displayed in the scatter plot (Fig. 11), but for MRD values in Fig. 13. At altitudes above 22 to 25 km, SCIAMACHY NO₂ shows a low bias compared with HALOE NO₂ for NH and SH high latitudes. A low bias in HALOE NO₂ v17 was discovered in Gordley et al. (1996) for altitudes below 25 km, and aerosols were reported as a major error source. For HALOE NO₂ v19, a comparison with the Shuttle-based FTIR-instrument ATMOS is done by Randall et al. (2002), which indicates that

the low bias of about 0.5 ppbv for HALOE at low altitudes was reduced to 0.2 to 0.3 ppbv in the new version. It is stated, that with the low NO₂ levels below 25 km, this can still result in a negative bias of up to 40%. In Borchini et al. (2007), a low bias or altitude mismatch for O₃ is reported at altitudes below 23 km in the tropics for HALOE v19. This indicates, that the positive bias of SCIAMACHY seen below 25 km is most probably due to quality issues of HALOE data. Additionally, HALOE NO₂ retrieval applies a correction for the diurnal effect error, which would lead to a negative bias of SCIAMACHY compared with HALOE if uncorrected.

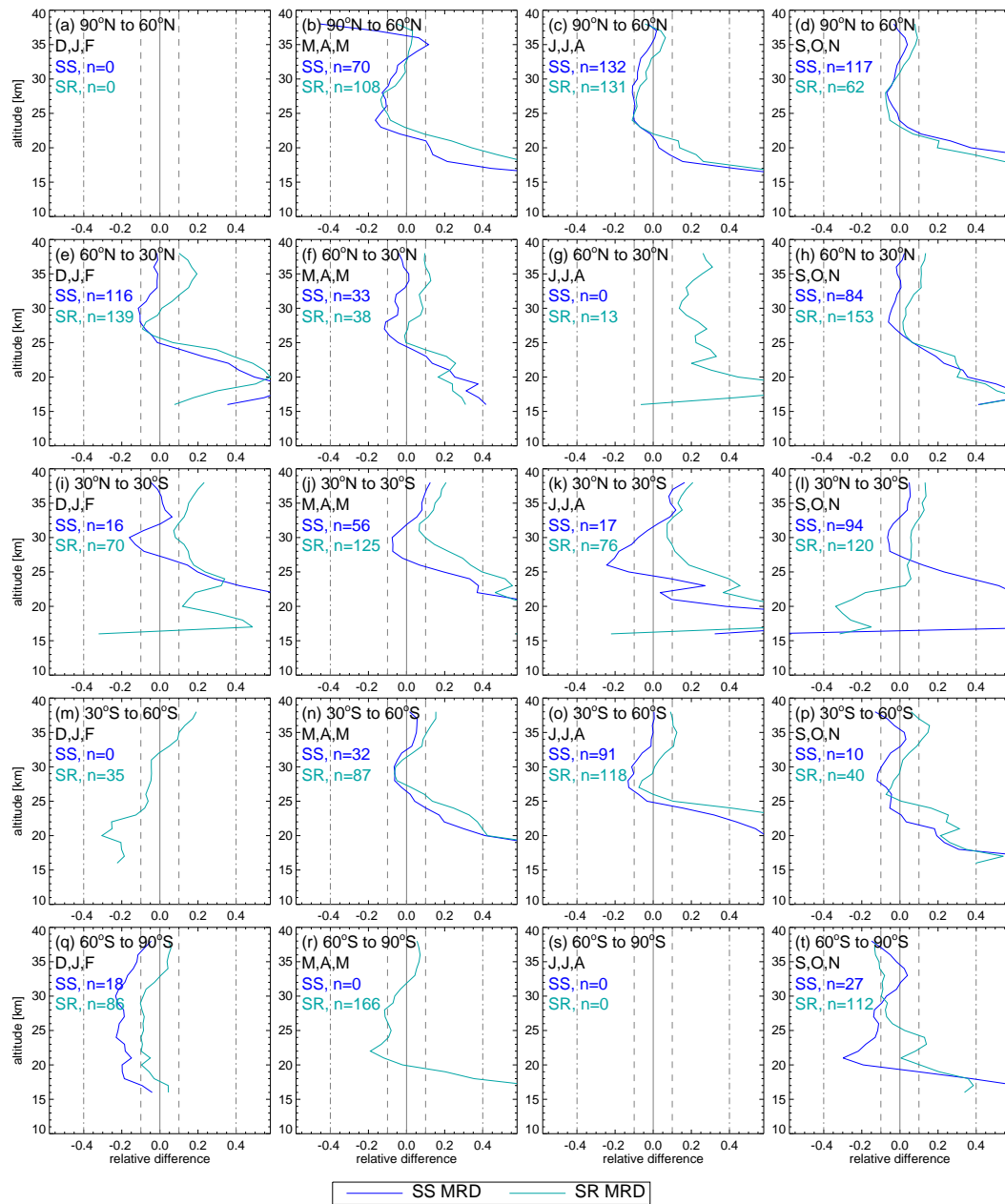


Fig. 13. MRDs between SCIAMACHY and photochemically corrected HALOE NO₂ profiles are displayed as blue (sunset) and cyan (sunrise) solid lines for each latitude and season.

The third instrument to compare with is ACE-FTS. Because of the mission time, the years 2004 and 2005 are chosen for investigation. In this comparison, 525 collocations in 2004 are used and 1143 in 2005, which represents the smallest dataset of the three instruments. Scatter plots are shown in Fig. 14 revealing generally high r^2 values, larger than 0.9 in all cases below 35 to 40 km (Both sunset and sunrise measurements are included).

Figure 15 shows the averaged NO₂ profiles in each latitude/season bin, where SCIAMACHY results are shown as

a black line with the standard deviations for the subset of collocations as a dashed black line. Photochemically corrected and averaged ACE-FTS NO₂ profiles are given as a green line, while the standard deviations for each subset of profiles are shown as dashed green lines. Contrary to HALOE and SAGE II, collocations are also available at 90° N to 60° N in NH winter and 60° S to 90° S in SH winter. About 50% of all collocations are found between 90° N to 60° N in just two seasons, namely, in March, April and May (487 collocations), and in September, October and November

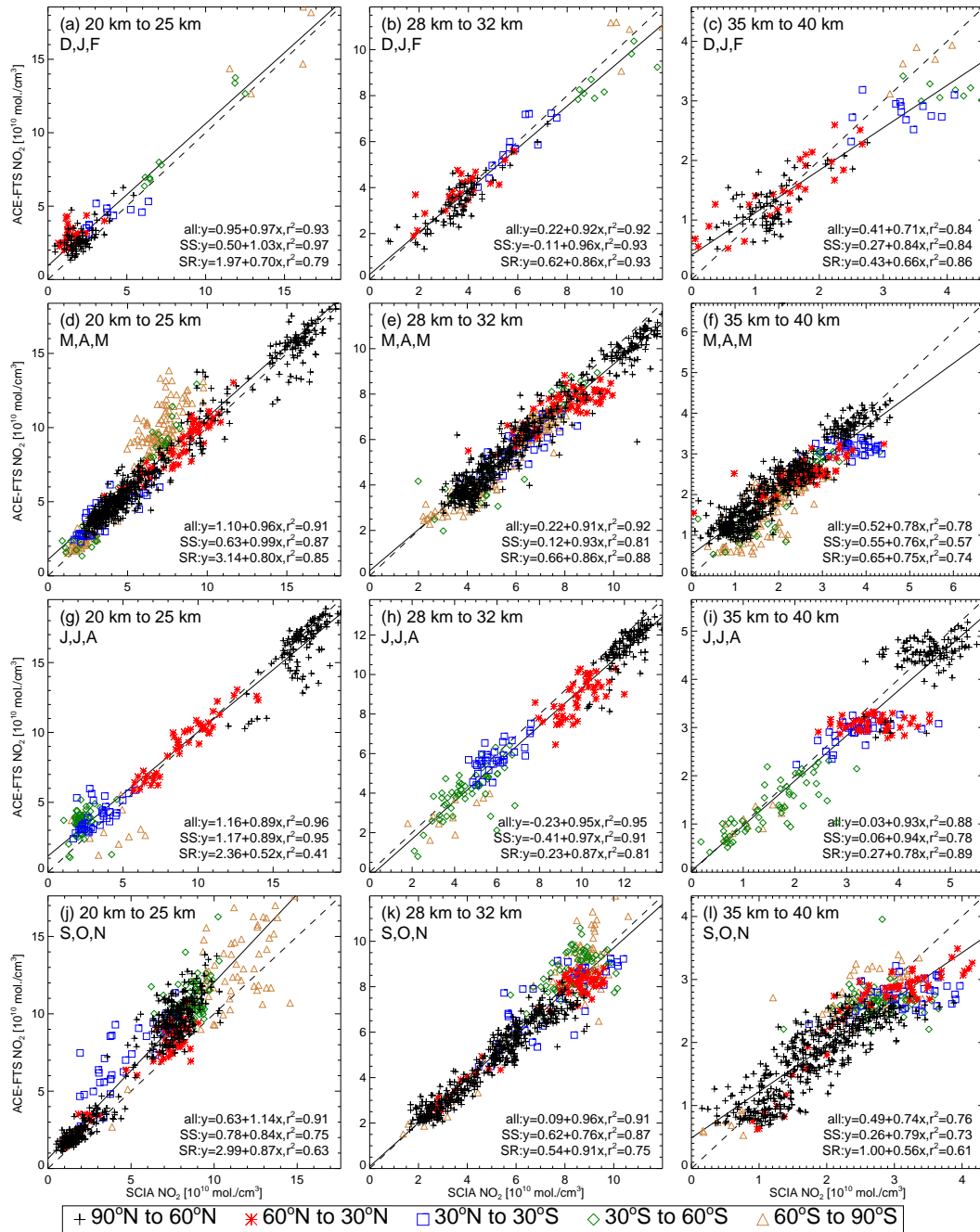


Fig. 14. Same as Fig. 8, but for ACE-FTS. Data sets from the years 2004 and 2005 are shown in this figure. 1668 collocation pairs are shown (817 for ACE-FTS sunset and 851 for sunrise).

(409 collocations). Two latitude/seasonal bins in the Southern Hemisphere contain less than 10 collocations in December, January and February. The summary of MRDs for SCIAMACHY to ACE-FTS comparisons is given in Table 4.

With the same method as applied for SAGE II, the possible influence from the diurnal effect error is removed from each photochemically corrected ACE-FTS profile, see Fig. 16. Although in many cases the MRD_{CORR} values are larger above

25 km, an considerable improvement below this altitude for both tropics and middle latitudes is seen for both sunset and sunrise measurements, i.e. MRD_{CORR} is closer to zero in most cases. Contrary to SAGE II, this correction can be regarded as an improvement for both sunset and sunrise ACE-FTS NO₂, at least at altitudes below 25 to 30 km. Also not considering the diurnal effect error correction, averaged MRD values for sunset and sunrise measurements do not show the

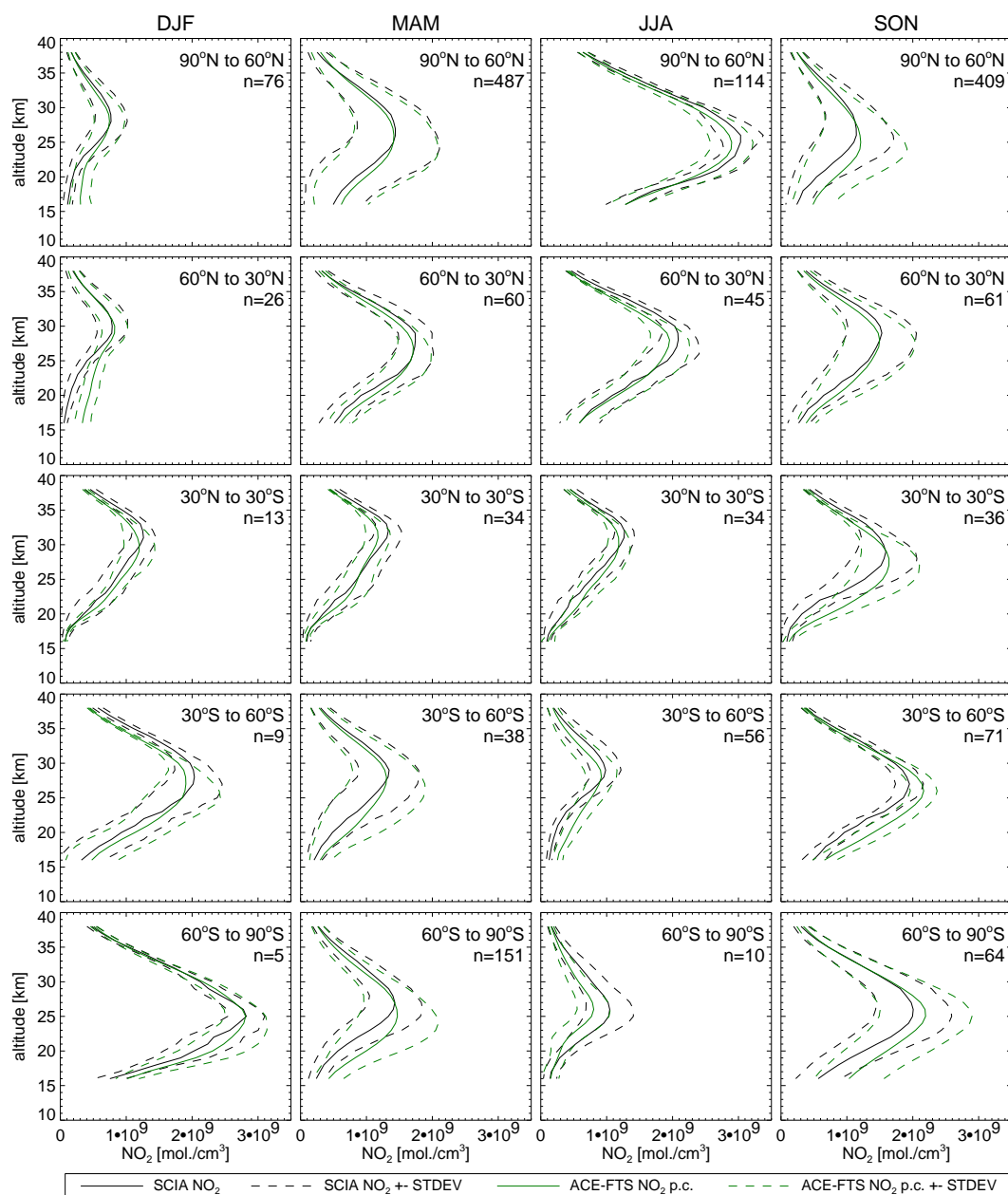


Fig. 15. Same as Fig. 9, but for ACE-FTS. Instead of 2003 and 2004, datasets from 2004 and 2005 are averaged in this figure.

large differences seen for SAGE II. However, the number of collocations, n , is low in many latitude/seasons bins for either sunset or sunrise measurements appears. Excluding 90° N to 60° N and 60° S to 90° S, where the assumption of low diurnal effect errors for SCIAMACHY is not valid, the MRD_{corr} values are given in Table 4.

In Kerzenmacher et al. (2008), ACE-FTS V2.2 NO₂ VMR profiles were compared with data from a number of instruments. It was found, that ACE-FTS NO₂ has a small negative bias (about 10 %) in the 23 to 40 km altitude range. This agrees well with the (varying) positive bias of SCIAMACHY

limb NO₂ in Fig. 16 for altitudes above 25 km. The negative bias below this altitude can be mostly attributed to the diurnal effect error. This statement might also be true for the NH and SH high latitudes (Fig. 15), but this cannot be analyzed with the present method.

3.4 Discussion

Summing up the results from the three instruments, the lowest MRDs are found at high latitudes and summer conditions (North and South) and all three instruments show a reasonable agreement with SCIAMACHY, although distinct

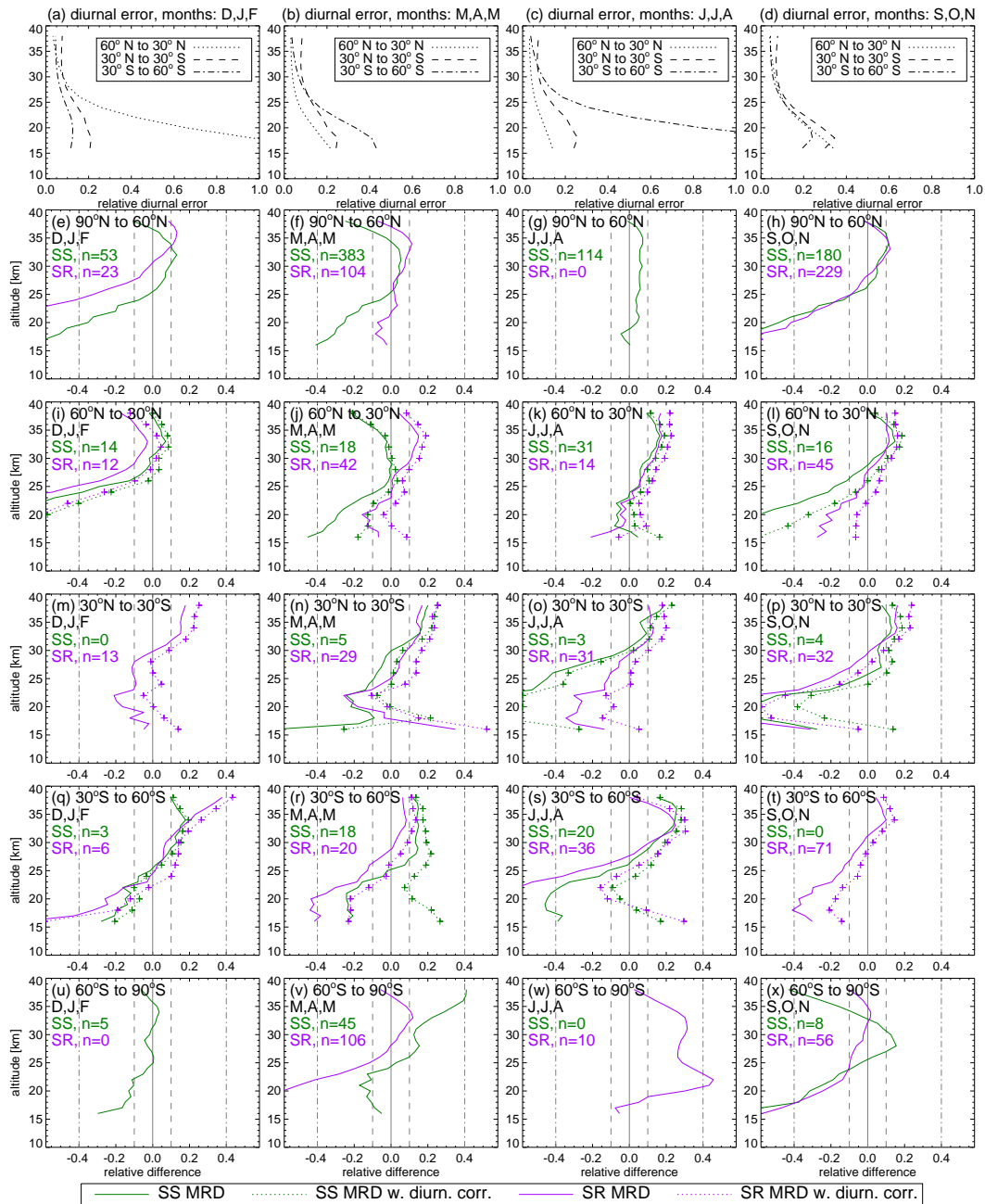


Fig. 16. For the latitude regions and seasons investigated in Fig. 15, the relative diurnal error for ACE-FTS measurements is estimated and averaged in panels (a) to (d). Panels (i) to (t) show estimates of how this error influences the MRD between photochemically corrected ACE-FTS and SCIAMACHY limb NO₂ amounts. The solid green lines shows the MRD of photochemically corrected NO₂ sunset profiles from ACE-FTS without the diurnal effect error with SCIAMACHY results, and the green dashed line with the diurnal effect error. The same calculations are performed for sunrise measurements, with MRD values shown as violet solid lines, and violet dashed for MRD_{CORR} values with considering the diurnal effect error.

features are seen. Higher NO₂ values at lower altitudes are one of the reasons for mostly smaller relative differences at high latitudes. Additionally, the SCIAMACHY measurements at high latitudes feature higher SZAs (about 70° to slightly below 90°) compared to measurements in the tropics,

where a SZA of 30° is common. This means a smaller photochemical correction of the profiles. Contrary to HALOE and SAGE II, collocations with ACE-FTS allow to compare NO₂ amounts during high latitudes winter (90° N to 60° N in D, J, F), i.e. for very low NO₂ amounts with maximum values

Table 2. Mean relative differences (MRD) for all SAGE II comparisons and for an altitude range from 20 to 40 km, respectively. Mean solar zenith angles SZA and mean local times \bar{t} for SCIAMACHY are given for each bin. MRD_{corr} represents comparisons, where an additional diurnal effect error correction has been applied where appropriate.

months	latitude range	SCIA SZAs	SCIA \bar{t} . a.m. (p.m.)	<i>n</i> SS/SR	MRD min/max/avg [%]			MRD _{corr} min/max/avg [%]	
					all	SS	SR	SS	SR
DJF	90° N–60° N			0/0	<i>n</i> < 10				
	60° N–30° N	55.9–76.8	10.0	83/119	–36/6/–11	–67/–13/–31	–8/24/8	–57/–11/–29	–21/59/19
	30° N–30° S	34.2–57.8	9.6	36/36	–2/13/5	–45/–6/–21	15/88/40	–32/–2/16	21/112/51
	30° S–60° S	50.1–59.0	8.7	0/27	–19/16/5	<i>n</i> < 10	–19/16/5	<i>n</i> < 10	–3/19/12
	60° S–90° S	50.3–89.7	7.8 (22.9)	0/200	–10/18/6	<i>n</i> < 10	–10/18/6		
MAM	90° N–60° N	55.7–86.9	11.3 (17.2)	129/0	–43/–6/–15	–43/–6/–15	<i>n</i> < 10		
	60° N–30° N	22.7–61.8	10.0	6/76	–2/14/7	<i>n</i> < 10	0/16/9	<i>n</i> < 10	0/26/15
	30° N–30° S	22.8–62.3	9.4	13/131	10/29/19	–70/4/–19	12/37/23	–48/8/–13	20/57/33
	30° S–60° S	58.3–84.5	8.8	100/67	–28/12/–3	–49/3/–13	–17/22/3	–24/6/–6	2/39/16
	60° S–90° S	73.3–80.7	7.3	0/6	<i>n</i> < 10	<i>n</i> < 10	<i>n</i> < 10		
JJA	90° N–60° N	39.1–87.2	11.3 (19.1)	317/0	–36/0/–8	–36/0/–8	<i>n</i> < 10		
	60° N–30° N	26.9–51.9	9.9	0/38	6/24/14	<i>n</i> < 10	6/25/15	<i>n</i> < 10	14/37/23
	30° N–30° S	24.6–61.6	9.4	22/113	1/32/16	–69/0/–22	5/50/25	–48/4/–17	14/74/37
	30° S–60° S	57.0–84.6	8.8	130/75	–52/1/–18	–66/–4/–24	–31/16/–6	–57/–2/–20	–40/65/9
	60° S–90° S			0/0	<i>n</i> < 10				
SON	90° N–60° N	54.6–87.3	11.1 (16.5)	135/0	–35/–4/–12	–35/–4/–12	<i>n</i> < 10		
	60° N–30° N	40.6–74.8	10.0	111/72	–23/5/–6	–44/–2/–16	–4/20/7	–31/–1/–12	5/36/17
	30° N–30° S	26.2–51.9	9.5	71/75	0/20/11	–37/7/–10	18/78/36	–20/11/–3	25/97/48
	30° S–60° S	39.1–75.1	8.6	0/72	–2/22/10	<i>n</i> < 10	–2/22/10	<i>n</i> < 10	–11/25/15
	60° S–90° S	47.6–89.7	8.2	0/76	–7/4/–1	<i>n</i> < 10	–7/4/–1		

Table 3. Same as Table 2, but for HALOE collocations. An altitude range from 20 to 40 km is covered. MRD_{corr} values are not given, as the diurnal effect error correction can not be applied for HALOE, as HALOE NO₂ is already corrected for this.

months	latitude range	SCIA SZAs	SCIA \bar{t} . a.m. (p.m.)	<i>n</i> SS/SR	MRD min/max/avg [%]		
					all	SS	SR
DJF	90° N–60° N			0/0	<i>n</i> < 10		
	60° N–30° N	54.9–75.9	10.0	116/139	–9/48/8	–11/42/2	–9/55/14
	30° N–30° S	28.4–55.3	9.4	16/70	3/34/16	–16/88/11	7/34/18
	30° S–60° S	31.1–50.8	8.8	0/35	–25/19/–1	<i>n</i> < 10	–25/19/–1
	60° S–90° S	46.8–72.8	8.0	18/86	–13/3/–6	–23/–3/–16	–10/6/–4
MAM	90° N–60° N	57.8–87.7	11.0 (18.9)	70/108	–46/16/–7	–70/12/–11	–18/24/–3
	60° N–30° N	38.5–61.4	10.0	33/38	–5/23/5	–12/23/–1	–1/26/9
	30° N–30° S	23.1–62.3	9.5	56/125	3/57/21	–8/59/12	7/56/26
	30° S–60° S	54.1–78.6	9.0	32/87	–6/37/10	–7/30/4	–6/40/12
	60° S–90° S	65.6–78.8	7.9	0/166	–19/7/–4	<i>n</i> < 10	–19/7/–4
JJA	90° N–60° N	40.4–87.1	10.8 (20.1)	132/131	–13/6/–5	–11/2/–6	–17/13/–3
	60° N–30° N	27.7–34.6	9.8	0/13	14/33/24	<i>n</i> < 10	14/33/24
	30° N–30° S	22.1–62.9	9.4	17/76	4/45/17	–24/27/2	7/52/21
	30° S–60° S	54.4–82.9	8.9	91/118	–10/78/12	–13/54/4	–8/102/20
	60° S–90° S			0/0	<i>n</i> < 10		
SON	90° N–60° N	55.6–69.8	11.0 (12.3)	117/62	–7/24/1	–7/26/1	–8/21/2
	60° N–30° N	40.5–72.0	10.0	84/153	–1/32/9	–6/33/4	2/32/12
	30° N–30° S	26.9–54.5	9.5	94/120	0/20/8	–6/82/14	–25/14/5
	30° S–60° S	29.4–68.1	9.0	10/40	–7/29/6	–18/18/–4	–7/31/8
	60° S–90° S	66.6–89.7	6.8	27/112	–13/6/–7	–30/4/–10	–13/14/–5

Table 4. Same as Table 2, but for ACE-FTS collocations. An altitude range from 20 to 40 km is covered.

months	latitude range	SCIA SZAs	SCIA $\bar{I}.t.$ a.m. (p.m.)	n SS/SR	MRD min/max/avg [%]			MRD _{corr} min/max/avg [%]	
					all	SS	SR	SS	SR
DJF	90° N–60° N	77.7–89.8	10.9 (12.7)	53/23	–51/11/–5	–32/13/–2	–90/13/–14		
	60° N–30° N	68.0–84.7	10.3	14/12	–90/3/–20	–75/7/–14	–105/–3/–28	–57/9/–9	–61/4/–17
	30° N–30° S	36.2–44.8	9.4	0/13	–21/18/1	$n < 10$	–21/18/1	$n < 10$	–5/25/11
	30° S–60° S	44.6–47.4	8.9	3/6	$n < 10$	$n < 10$	$n < 10$	$n < 10$	$n < 10$
	60° S–90° S	48.9–58.0	8.2	5/0	$n < 10$	$n < 10$	$n < 10$		
MAM	90° N–60° N	44.4–89.6	11.1 (15.3)	385/104	–28/6/–3	–35/5/–6	–16/11/3		
	60° N–30° N	27.0–59.8	10.2	18/42	–12/10/2	–28/1/–9	–8/15/6	–32/3/–8	–4/19/9
	30° N–30° S	25.1–50.2	9.5	5/29	–25/17/5	$n < 10$	–26/17/5	$n < 10$	–11/25/14
	30° S–60° S	50.8–89.1	8.7	18/20	–33/10/–1	–24/15/6	–35/8/–4	0/22/14	–22/14/3
	60° S–90° S	66.4–89.2	7.8	45/106	–48/14/–3	–17/41/16	–50/12/–6		
JJA	90° N–60° N	39.8–87.1	10.4 (20.0)	114/0	–8/7/4	–8/7/4	$n < 10$		
	60° N–30° N	26.7–41.8	10.0	31/14	–7/17/8	–7/16/8	–5/18/10	0/19/10	5/23/16
	30° N–30° S	26.8–50.5	9.4	3/31	–33/13/–2	$n < 10$	–30/13/–1	$n < 10$	–13/20/7
	30° S–60° S	60.7–89.0	8.8	20/36	–63/24/–3	–43/26/4	–74/25/–7	–9/28/12	–23/31/6
	60° S–90° S	83.7–88.7	8.4	0/10	–4/46/26	$n < 10$	–4/46/26		
SON	90° N–60° N	55.6–88.3	11.0 (12.8)	180/229	–34/11/–3	–42/11/–3	–33/12/–3		
	60° N–30° N	40.5–81.2	10.3	16/45	–18/12/2	–50/15/–5	–15/12/3	–32/19/0	–6/16/9
	30° N–30° S	26.6–33.6	9.2	4/32	–69/16/–7	$n < 10$	–70/16/–7	$n < 10$	–58/24/0
	30° S–60° S	33.8–53.6	8.8	0/71	–30/10/–5	$n < 10$	–30/10/–5	$n < 10$	–18/15/0
	60° S–90° S	51.4–86.3	8.2	8/56	–19/1/–7	$n < 10$	–19/2/–7		

smaller than 1.0×10^9 molec cm^{–3} and large SCIAMACHY SZAs (77.7° to 89.8°). In this case, the MRDs are comparably high (–51 % to 11 % at 20 to 40 km), see Table 4, which means that large SZAs do not automatically yield low MRDs.

NO₂ concentrations change rapidly at daybreak and change much less during the day at most altitudes investigated here. Still, the photochemical correction method can not be excluded as a significant error source. Also, the altitude range of the three occultation instruments varies and the number of averaged profiles is also smaller at low altitudes. For example, 572 HALOE profiles are averaged at most altitudes in the tropics. This number decreases to 563 at 18 km and further to only 492 valid profiles at 15 km. However, these numbers are still reasonably high. It is worth mentioning that the profiles were not smoothed, i.e. differences in resolution have not been accounted for. Also, estimating the change of including the diurnal effect error in photochemically corrected profiles results in improvements for sunset measurements of SAGE II and both sunset and sunrise measurements for ACE-FTS at 25 km and below, where the diurnal effect error shows the highest values.

Table 5 presents MRDs for all instruments (as given in Tables 2 to 4) averaged either over all seasons or over all latitude bins. In addition, the MRDs averaged over the whole globe all seasons (i.e. the complete data set) are given as a reference for 20 to 40 km and 25 to 35 km. If these values are considered, the reader is strongly recommended to take the MRDs of the individual latitude/seasonal bins into account, since negative and positive relative differences may cancel

each other out. This is especially true for the MRDs in the all latitudes/all seasons scenario, which results in MRDs smaller than 20 % or even 10 % as a consequence of averaging. In the right column of Table 5, standard deviations for the relative differences of all altitudes and collocations are given for each subset. Both at 90° N to 60° N and in NH summer, standard deviations of less than 20 % are seen for all instruments. In the tropics, the standard deviations can exceed 30 %.

MRD values obtained after applying the diurnal effect error correction are denoted as MRD_{corr} in Tables 2 and 4. As the diurnal scaling only improves the agreement below 25 km (with the exception of SAGE II sunrise), the MRD_{corr} values for 20 to 40 km are not always smaller than those without the diurnal effect error correction.

To estimate the bias of SCIAMACHY NO₂, the MRDs at 25 to 35 km and the case of all seasons and all latitudes are investigated. It should be noted, that the bias for individual seasons and latitudes may be different. Below 25 km, diurnal effect errors and other error sources have a strong influence on the result, so the bias is difficult to determine at these altitudes. For SAGE II sunset results, an average MRD of –6 % remains, i.e. photochemically corrected SAGE II NO₂ amounts are higher than SCIAMACHY NO₂ on average. In Bracher et al. (2005), SAGE II NO₂ values were found to be high in comparison to SCIAMACHY with MRDs of –10 % to –35 % between 20 and 38 km. However, these values apply only to a subset of measurements with a SZA range of 60 to 70°, only sunset measurements and only for the year 2003. If we limit the collocations for the SAGE II comparisons by

Table 5. Mean relative differences (MRD) for all comparisons at 20 to 40 km. Standard deviations (STDEV) are calculated for each subset of collocations in the given altitude range.

months	latitude range	MRD min/max/avg [%]			STDEV [%]
		all	SS	SR	
SAGE II					
all	90° N–60° N	–37/–3/–10	–37/–3/–10	<i>n</i> = 0	14
all	60° N–30° N	–17/8/–2	–52/–6/–21	1/18/9	29
all	30° N–30° S	4/24/14	–46/2/–15	12/54/28	34
all	30° S–60° S	–27/8/–5	–60/–2/–20	–13/18/4	28
all	60° S–90° S	–8/14/5	<i>n</i> = 0	–8/14/5	19
DJF	90° N–90° S	–13/10/1	–60/–10/–28	–7/19/8	25
MAM	90° N–90° S	–9/7/0	–33/–4/–13	2/23/12	26
JJA	90° N–90° S	–22/2/–4	–36/–2/–10	1/27/14	20
SON	90° N–90° S	–9/6/–2	–24/–1/–12	4/22/11	24
all	90° N–90° S	–11/5/–2	–33/–4/–12	0/22/11	23
	all, 25 to 35 km	–4/5/1	–10/–4/–6	3/18/9	17
HALOE					
all	90° N–60° N	–19/12/–4	–22/8/–6	–13/17/–2	17
all	60° N–30° N	–4/35/8	–9/34/2	–1/36/13	29
all	30° N–30° S	3/35/15	–8/68/12	7/31/16	33
all	30° S–60° S	–7/32/7	–11/43/3	–5/28/9	30
all	60° S–90° S	–11/0/–5	–24/–5/–13	–10/1/–4	22
DJF	90° N–90° S	–7/9/2	–14/14/–4	–4/14/4	27
MAM	90° N–90° S	–6/15/2	–29/18/–3	–4/13/4	25
JJA	90° N–90° S	–8/14/0	–12/5/–5	–4/25/5	18
SON	90° N–90° S	–4/12/3	–7/18/1	–2/13/5	25
all	90° N–90° S	–6/12/2	–10/12/–3	–3/13/4	24
	all, 25 to 35 km	–6/6/–2	–10/1/–6	–3/8/1	17
ACE-FTS					
all	90° N–60° N	–17/8/–1	–20/6/–1	–19/11/–1	18
all	60° N–30° N	–15/12/3	–16/10/1	–14/13/4	17
all	30° N–30° S	–42/15/–2	–47/16/–3	–41/15/–2	28
all	30° S–60° S	–34/14/–2	–28/20/5	–35/12/–4	24
all	60° S–90° S	–33/10/–3	–14/26/10	–35/8/–5	22
DJF	90° N–90° S	–38/10/–3	–27/10/–2	–56/15/–6	27
MAM	90° N–90° S	–20/9/–2	–27/6/–4	–18/12/1	20
JJA	90° N–90° S	–3/12/5	–5/10/5	–27/17/3	14
SON	90° N–90° S	–31/10/–3	–42/11/–3	–30/10/–3	21
all	90° N–90° S	–20/10/–1	–15/8/0	–25/12/–1	20
	all, 25 to 35 km	–2/10/5	3/8/6	–6/12/4	13

applying similar restrictions, the MRD values lie between –7 % and –30 %, on average –17 %. If the MRDs are normalized with respect to the particular SAGE II profile as in Bracher et al. (2005), the MRD values lie between –8 % and –39 %, which agree very well with the known results.

For HALOE, a global comparison including all seasons at 25 to 35 km shows a small average MRD of only –2 %. In Gordley et al. (1996), no obvious bias was found between

25 and 40 km. If the same calculation is done for ACE-FTS (MRD globally, all seasons, 25 to 35 km), a 5 % average MRD is found. For altitudes between 25 and 40 km, a negative bias of about 10 % is estimated by Kerzenmacher et al. (2008) for ACE-FTS, which agrees qualitatively with our results. From the results of the three instruments, a low bias for SCIAMACHY NO₂ between 0 and –5 % is most likely, although it is strongly recommended to not underestimate the

influence of the uneven distribution of collocations in each validation set on this result.

Regarding standard deviations, these are found for all three satellites to be smaller than 20 % in the global/biannual mean comparison at 20 to 40 km, and smaller than 17 % between 25 and 35 km. In NH summer (June, July and August), standard deviations are less than 20 % globally, which is also the case for all season subsets between 90° N and 60° N, while between 60° S and 90° S standard deviations are less than 22 %. However, in tropics, standard deviations can exceed 30 %.

4 Conclusions

This work gives an overview of the performance and sensitivity of SCIAMACHY NO₂ limb retrieval relying mainly on a range of occultation instruments (SAGE II, HALOE, ACE-FTS). To address the problem of high diurnal variability of NO₂, photochemical corrections are applied. The diurnal effect error that originates from changing SZA along the line of sight for individual measurements is also discussed.

In this work, thousands of profile pairs are investigated after applying collocation criteria, using data from each instrument obtained during two years over the whole globe. As NO₂ amounts are highly variable dependent on latitude and season, the data are gridded into five latitude and four seasonal bins, and the results for each available latitude/season bin are presented.

In comparison with the three occultation instruments used for validation, SCIAMACHY NO₂ shows a high bias with respect to photochemically corrected SAGE II sunrise NO₂ amounts, but a low bias compared with SAGE II sunset NO₂ values. As the SAGE II sunset results are regarded as more reliable, a low NO₂ bias (or mean relative difference about -6 % at 25 to 35 km) can be attributed for SCIAMACHY in this comparison, in line with former results. For HALOE, a small MRD of -2 % is found in a global scenario including all datasets. In contrast, the overall average MRD for ACE-FTS is about 5 %. However, ACE-FTS is known to have a small negative bias of about 10 %. Although these comparisons suggest a low NO₂ bias (-5 to 0 %) for SCIAMACHY, it is recommended to read the results for individual latitude/season bins presented in this study.

The standard deviations of the relative differences are found to be smaller than 20 % in many scenarios (e.g. 90° N to 60° N and all seasons), but can exceed 30 % in the tropics. For the globally averaged complete dataset, the standard deviations are below 22 % between 20 and 40 km, and below 17 % at 25 to 35 km.

Due to different operation times of the instruments, the years 2004 and 2005 are investigated for ACE-FTS, while SAGE II and HALOE analysis is done for 2003 and 2004. Altitudes lower than 20 km are not taken into account for the scatter plots or the calculation of MRD. However, the

error analysis shows that uncertainties from different sources including aerosols and clouds can have a significant impact below this altitude. Retrieval and validation of NO₂ in limb mode at 15 km and below is a challenge that is beyond the scope of this work, but is expected to provide interesting insights in the composition and sources of atmospheric pollution.

The data basis allowed us a closer look in different latitudinal regions and seasons. Compared with high latitudes (90° N to 60° N, 60° S to 90° S), the relative differences in NO₂ amounts are higher in the tropics (30° N to 30° S) for all instruments used for validation. Possible reasons for this are most likely the diurnal effect error, low NO₂ values, and small SZAs for SCIAMACHY, which may result in a less accurate photochemical correction.

To conclude, this work is expected to contribute to investigations of NO₂ content and emissions, for which validated long-term data sets are of great importance.

Acknowledgements. We are thankful to ECMWF for providing pressure and temperature information (ECMWF Special Project SPDECIDIO) for this study. Some data shown here were calculated on German HLRN (High-Performance Computer Center North). Services and support provided by the Atmospheric Chemistry Experiment (ACE), also known as SCISAT, a Canadian-led mission mainly supported by the Canadian Space Agency and the Natural Sciences and Engineering Research Council of Canada, are greatly appreciated. Our gratitude also goes to the HALOE science and data processing teams for providing the profiles used in this study. We wish to thank the NASA Langley Research Center (NASA-LaRC) and the NASA Langley Radiation and Aerosols Branch for making it possible for us to work with SAGE II data sets. This work was funded in parts by the European Commission FP7 project QUANTIFY, the DLR project SADOS (FKZ 50EE0727), by ESA through the SCIAMACHY Quality Working Group and by the University and State of Bremen.

Edited by: P. K. Bhartia

References

- Backus, G. and Gilbert, F.: Uniqueness in the inversion of inaccurate gross earth data, *Philos. T. Roy. Soc. Lond. A*, 266, 123–192, 1970.
- Bernath, P. F., McElroy, C. T., Abrams, M. C., Boone, C. D., Butler, M., Camy-Peyret, C., Carleer, M., Clerbaux, C., Coheur, P.-F., Colin, R., DeCola, P., DeMazière, M., Drummond, J. R., Dufour, D., Evans, W. F. J., Fast, H., Fussen, D., Gilbert, K., Jennings, D. E., Llewellyn, E. J., Lowe, R. P., Mahieu, E., McConnell, J. C., McHugh, M., McLeod, S. D., Michaud, R., Midwinter, C., Nassar, R., Nichituu, F., Nowlan, C., Rinsland, C. P., Rochon, Y. J., Rowlands, N., Semeniuk, K., Simon, P., Skelton, R., Sloan, J. J., Soucy, M.-A., Strong, K., Tremblay, P., Turnbull, D., Walker, K. A., Walkty, I., Wardle, D. A., Wehrle, V., Zander, R., and Zou, J.: Atmospheric chemistry experiment (ACE): mission overview, *Geophys. Res. Lett.*, 32, L15S01, doi:10.1029/2005GL022386, 2005.

- Bogumil, K., Orphal, J., Voigt, S., Bovensmann, H., Fleischmann, O. C., Hartmann, M., Homann, T., Spietz, P., Vogel, A., and Burrows, J. P.: Reference spectra of atmospheric trace gases measured with the SCIAMACHY PFM satellite spectrometer, in: Proc. 1st Europ. Sympos. Atmos. Meas. from Space (ESAMS-99), 2, 443–447, ESA-ESTEC, Noordwijk, 1999.
- Boone, C., Nassar, R., Walker, K., Rochon, Y., McLeod, S., Rinsland, C., and Bernath, P.: Retrievals for the atmospheric chemistry experiment Fourier-transform spectrometer, *Appl. Optics*, 44, 7218–7231, 2005.
- Borchi, F. and Pommereau, J.-P.: Evaluation of ozonesondes, HALOE, SAGE II and III, Odin-OSIRIS and -SMR, and ENVISAT-GOMOS, -SCIAMACHY and -MIPAS ozone profiles in the tropics from SAOZ long duration balloon measurements in 2003 and 2004, *Atmos. Chem. Phys.*, 7, 2671–2690, doi:10.5194/acp-7-2671-2007, 2007.
- Bovensmann, H., Burrows, J. P., Buchwitz, M., Frerick, J., Noël, S., Rozanov, V., Chance, K., and Goede, A.: SCIAMACHY: Mission objectives and measurement modes, *J. Atmos. Sci.*, 56, 127–150, 1999.
- Bracher, A., Weber, M., Bramstedt, K., Tellmann, S., and Burrows, J. P.: Long-term global measurements of ozone profiles by GOME validated with SAGE II considering atmospheric dynamics, *J. Geophys. Res.*, 109, D20308, doi:10.1029/2004JD004677, 2004.
- Bracher, A., Sinnhuber, M., Rozanov, A., and Burrows, J. P.: Using a photochemical model for the validation of NO₂ satellite measurements at different solar zenith angles, *Atmos. Chem. Phys.*, 5, 393–408, doi:10.5194/acp-5-393-2005, 2005.
- Brohede, S., Haley, C., McLinden, C., Sioris, C., Murtagh, D., Petelina, S. V., Llewellyn, E. J., Bazureau, A., Goutail, F., Randall, C., Lumpe, J. D., Taha, G., Thomasson, L. W., and Gordley, L. L.: Validation of Odin/OSIRIS stratospheric NO₂ profiles, *J. Geophys. Res.*, 112, D07310, doi:10.1029/2006JD007586, 2007.
- Burrows, J. P., Hötze, E., Goede, A., Visser, H., and Fricke, W.: SCIAMACHY – scanning imaging absorption spectrometer for atmospheric cartography, *Acta Astronaut.*, 35, 445–451, 1995.
- Chu, W. P., McCormick, M. P., Lenoble, J., Brogniez, C., and Pruvost, P.: SAGE II inversion algorithm, *J. Geophys. Res.*, 94, 8339–8351, 1989.
- Crutzen, P.: The influence of nitrogen oxides on the atmospheric ozone content, *Q. J. Roy. Meteorol. Soc.*, 96, 320–325, 1970.
- Cunnold, D. M., Zawodny, J. M., Chu, W. P., Pommereau, J. P., Goutail, F., Lenoble, J., McCormick, M. P., Veiga, R. E., Murcray, D., Iwagami, N., Iwagami, N., Shibasaki, K., Simon, P. C., and Peetermans, W.: Validation of SAGE II NO₂ Measurements, *J. Geophys. Res.*, 96, 12913–12925, 1991.
- Doicu, A., Hilgers, S., von Barmen, A., Rozanov, A., Eichmann, K.-U., von Savigny, C., and Burrows, J. P.: Information Operator Approach and iterative regularization methods for atmospheric remote sensing, *J. Quant. Spectrosc. Ra.*, 103, 340–350, 2007.
- Eichmann, K.-U., von Savigny, C., Reichl, P., Robert, C., Steinwagner, J., Bovensmann, H., and Burrows, J. P.: SCODA: SCIAMACHY Cloud Detection Algorithm from Limb Radiance Measurements – Algorithm theoretical basis document, Tech. rep., Institute of Environmental Physics, University of Bremen, unpublished technical document, 2009.
- Gordley, L. L., Russell III, J. M., Mickley, L. J., Frederick, J. E., Park, J. H., Stone, K. A., Beaver, G. M., McInemey, J. M., Deaver, L. E., Toon, G. C., Murcray, F. J., Blatherwick, R. D., Gunson, M. R., Abbatt, J. P. D., Mauldin III, R. L., Mount, G. H., Sen, B., and Blavier, J.-F.: Validation of nitric oxide and nitrogen dioxide measurements made by the Halogen Occultation Experiment for UARS platform, *J. Geophys. Res.-Atmos.*, 101, 10241–10266, 1996.
- Haley, C. S., Brohede, S. M., Sioris, C. E., Griffioen, E., Murtagh, D. P., McDade, I. C., Eriksson, P., Llewellyn, E. J., Bazureau, A., and Goutail, F.: Retrieval of stratospheric O₃ and NO₂ profiles from Odin Optical Spectrograph and Infrared Imager System (OSIRIS) limb-scattered sunlight measurements, *J. Geophys. Res.*, 109, D16303, doi:10.1029/2004JD004588, 2004.
- Hervig, M. and McHugh, M.: Cirrus detection using HALOE measurements, *Geophys. Res. Lett.*, 26, 719–722, 1999.
- Hoinka, K.: Statistics of the global tropopause pressure, *Mon. Weather Rev.*, 126, 3303–3325, 1998.
- Hoogen, R., Rozanov, V. V., and Burrows, J. P.: Ozone profiles from GOME satellite data: Algorithm description and first validation, *J. Geophys. Res.*, 104, 8263–8280, doi:10.1029/1998JD100093, 1999.
- Kerzenmacher, T., Wolff, M. A., Strong, K., Dupuy, E., Walker, K. A., Amekudzi, L. K., Batchelor, R. L., Bernath, P. F., Berthet, G., Blumenstock, T., Boone, C. D., Bramstedt, K., Brogniez, C., Brohede, S., Burrows, J. P., Catoire, V., Dodion, J., Drummond, J. R., Dufour, D. G., Funke, B., Fussen, D., Goutail, F., Griffith, D. W. T., Haley, C. S., Hendrick, F., Höpfner, M., Huret, N., Jones, N., Kar, J., Kramer, I., Llewellyn, E. J., López-Puertas, M., Manney, G., McElroy, C. T., McLinden, C. A., Melo, S., Mikuteit, S., Murtagh, D., Nichitiu, F., Notholt, J., Nowlan, C., Piccolo, C., Pommereau, J.-P., Randall, C., Raspollini, P., Rindolfi, M., Richter, A., Schneider, M., Schrems, O., Silicani, M., Stiller, G. P., Taylor, J., Tétard, C., Toohey, M., Vanhellemont, F., Warneke, T., Zawodny, J. M., and Zou, J.: Validation of NO₂ and NO from the Atmospheric Chemistry Experiment (ACE), *Atmos. Chem. Phys.*, 8, 5801–5841, doi:10.5194/acp-8-5801-2008, 2008.
- Kneizys, F. X., Shettle, E. P., Abreu, L. W., Chetwynd, J. H., and Anderson, G. P.: Users Guide to LOWTRAN 7, Tech. rep., Air Force Geophysics Lab HANSCOM AFB MA, USA, <http://handle.dtic.mil/100.2/ADA206773> (last access: 19 April 2012), 1988.
- Kozlov, V.: Design of experiments related to the inverse of mathematical physics, in: *Mathematical Theory of Experiment Design*, edited by: Ermakov, C. M., Nauka, Moscow, 216–246, 1983.
- McLinden, C., Olsen, S. C., Hannegan, B., Wild, O., Prather, M. J., and Sundet, J.: Stratospheric ozone in 3-D models: A simple chemistry and the cross-tropopause flux, *J. Geophys. Res.*, 105, 14653, doi:10.1029/2000JD900124, 2000.
- McLinden, C., Haley, C., and Sioris, C.: Diurnal effects in limb scatter observations, *J. Geophys. Res.*, 111, D14302, doi:10.1029/2005JD006628, 2006.
- Montzka, S. A., Reimann, S., Engel, A., Krüger, K., O’Doherty, S., Sturges, W. T., Blake, D., Dorf, M., Fraser, P., Froidevaux, L., Jucks, K., Kreher, K., Kurylo, M. J., Mellouski, A., Miller, J., Nielsen, O.-J., Orkin, V. L., Prinn, R. G., Rhee, R., Santee, M. L., Stohl, A., and Verdonik, D.: Ozone-Depleting Substances (ODSs) and Related Chemicals, in: *Scientific Assessment of*

- Ozone Depletion: 2010, Global Ozone Research and Monitoring Project-Report No. 52, chap. 1, World Meteorological Organization, Geneva, Switzerland, 79–80, 2011.
- Noël, S., Bovensmann, H., Burrows, J., Frerick, J., Chance, K., Goede, A., and Müller, C.: SCIAMACHY instrument on ENVISAT-1, in: Proceedings of SPIE, vol. 3498, p. 94, 1998.
- Portmann, R. W., Brown, S. S., Gierczak, T., Talukdar, R. K., Burkholder, J. B., and Ravishankara, A. R.: Role of nitrogen oxides in the stratosphere: A reevaluation based on laboratory studies, *Geophys. Res. Lett.*, 26, 2387–2390, 1999.
- Prather, M.: Catastrophic loss of stratospheric ozone in dense volcanic clouds, *J. Geophys. Res.*, 97, 10187, doi:10.1029/92JD00845, 1992.
- Randall, C. E., Lumpe, J. D., Bevilacqua, R. M., Hoppel, K. W., Shettle, E. P., Rusch, D. W., Gordley, L. L., Kreher, K., Pfeilsticker, K., Boesch, H., Toon, G., Goutail, F., and Pommereau, J.-P.: Validation of POAM III NO₂ measurements, *J. Geophys. Res.*, 107, 4432, doi:10.1029/2001JD001520, 2002.
- Ravishankara, A. R., Daniel, J. S., and Portmann, R. W.: Nitrous oxide (N₂O): The dominant ozone-depleting substance emitted in the 21st century, *Science*, 326, 123–125, 2009.
- Rodgers, C. D.: Inverse Methods for Atmospheric Sounding, vol. 2 of Series on Atmospheric, Oceanic and Planetary Physics, World Scientific, 2000.
- Rozanov, A.: Sciatran – Radiative transfer model and retrieval algorithm, <http://www.iup.uni-bremen.de/sciatran/> (last access: 19 April 2012), 2012.
- Rozanov, A., Bovensmann, H., Bracher, A., Hrechanyy, S., Rozanov, V., Sinnhuber, M., Stroh, F., and Burrows, J.: NO₂ and BrO vertical profile retrieval from SCIAMACHY limb measurements: Sensitivity studies, *Adv. Space Res.*, 36, 846–854, 2005.
- Rozanov, A., Kühl, S., Doicu, A., McLinden, C., Pukite, J., Bovensmann, H., Burrows, J. P., Deutschmann, T., Dorf, M., Goutail, F., Grunow, K., Hendrick, F., von Hobe, M., Hrechanyy, S., Lichtenberg, G., Pfeilsticker, K., Pommereau, J. P., Van Roozendaal, M., Stroh, F., and Wagner, T.: BrO vertical distributions from SCIAMACHY limb measurements: comparison of algorithms and retrieval results, *Atmos. Meas. Tech.*, 4, 1319–1359, doi:10.5194/amt-4-1319-2011, 2011.
- Russel III, J. M. and Remsberg, E. E.: The HALogen Occultation Experiment (HALOE), <http://haloe.gats-inc.com> (last access: 19 April 2012), 2012.
- Russell III, J. M., Gordley, L. L., Park, J. H., Drayson, S. R., Hesketh, W. D., Cicerone, R. J., Tuck, A. F., Frederick, J. E., Harries, J. E., and Crutzen, P. J.: The halogen occultation experiment, *J. Geophys. Res.-Atmos.*, 98, 10777–10797, 1993.
- Sioris, C. E., Haley, C. S., McLinden, C. A., von Savigny, C., McDade, I. C., McConnell, J. C., Evans, W. F. J., Lloyd, N. D., Llewellyn, E. J., Chance, K. V., Kurosu, T. P., Murtagh, D., Frisk, U., Pfeilsticker, K., Bosch, H., Weidner, F., Strong, K., Stegman, J., and Megie, G.: Stratospheric profiles of nitrogen dioxide observed by Optical Spectrograph and Infrared Imager System on the Odin satellite, *J. Geophys. Res.*, 108, 4215, doi:10.1029/2002JD002672, 2003.
- Sonkaew, T.: Quantification of the chemical ozone loss in the northern and southern polar vortices using SCIAMACHY limb measurements, Ph.D. thesis, University of Bremen, Bremen, 2010.
- von Savigny, C., Ulasi, E. P., Eichmann, K.-U., Bovensmann, H., and Burrows, J. P.: Detection and mapping of polar stratospheric clouds using limb scattering observations, *Atmos. Chem. Phys.*, 5, 3071–3079, doi:10.5194/acp-5-3071-2005, 2005.
- von Savigny, C., Rozanov, A., Bovensmann, H., Noël, S., Gottwald, M., Slijkhuis, S., and Burrows, J.: Studying Envisat attitude with SCIAMACHY limb-scatter measurements, in: Proceedings of the Envisat Symposium, 2007.
- von Savigny, C., Bovensmann, H., Bramstedt, K., Dikty, S., Ebojje, F., Jones, A., Noël, S., Rozanov, A., and Sinnhuber, B.-M.: Indications for long-term trends and seasonal variations in the SCIAMACHY Level 1 version 6.03 tangent height information, Tech. rep., technical note TN-IUP-scia-pointing-2009-01 Issue 2, Institute of Environmental Physics, University of Bremen, 2009.
- Walker, K. A., Randall, C. E., Trepte, C. R., Boone, C. D., and Bernath, P. F.: Initial validation comparisons for the Atmospheric Chemistry Experiment (ACE-FTS), *Geophys. Res. Lett.*, 32, L16S04, doi:10.1029/2005GL022388, 2005.
- Wetzel, G., Bracher, A., Funke, B., Goutail, F., Hendrick, F., Lambert, J.-C., Mikuteit, S., Piccolo, C., Pirre, M., Bazureau, A., Belotti, C., Blumenstock, T., De Mazière, M., Fischer, H., Huret, N., Ionov, D., López-Puertas, M., Maucher, G., Oelhaf, H., Pommereau, J.-P., Ruhnke, R., Sinnhuber, M., Stiller, G., Van Roozendaal, M., and Zhang, G.: Validation of MIPAS-ENVISAT NO₂ operational data, *Atmos. Chem. Phys.*, 7, 3261–3284, doi:10.5194/acp-7-3261-2007, 2007.